ϵ_K at next-to-next-to-leading order: The charm-top-quark contribution

Joachim Brod[1,2,3] and Martin Gorbahn[2,3]

[1]*Institut für Theoretische Teilchenphysik, Universität Karlsruhe, D-76128 Karlsruhe, Germany*
[2]*Excellence Cluster Universe, Technische Universität München, Boltzmannstraße 2, D-85748 Garching*
[3]*Institute for Advanced Study, Technische Universität München, Arcisstraße 21, D-80333 München, Germany*

(Received 12 July 2010; published 18 November 2010)

We perform a next-to-next-to-leading order QCD analysis of the charm-top-quark contribution η_{ct} to the effective $|\Delta S| = 2$ Hamiltonian in the standard model. η_{ct} represents an important part of the short distance contribution to the parameter ϵ_K. We calculate the three-loop anomalous dimension of the leading operator $\tilde{Q}_{S2}$, the three-loop mixing of the current-current and penguin operators into $\tilde{Q}_{S2}$, and the corresponding two-loop matching conditions at the electroweak, the bottom-quark, and the charm-quark scale. As our final numerical result we obtain $\eta_{ct} = 0.496 \pm 0.047$, which is roughly 7% larger than the next-to-leading-order (NLO) value $\eta_{ct}^{\mathrm{NLO}} = 0.457 \pm 0.073$. This results in a prediction for $|\epsilon_K| = (1.90 \pm 0.26) \times 10^{-3}$, which corresponds to an enhancement of approximately 3% with respect to the value obtained using η_{ct}^{NLO}.

DOI: 10.1103/PhysRevD.82.094026 PACS numbers: 13.25.Es, 12.38.Bx, 12.15.Hh

I. INTRODUCTION

Indirect *CP* violation in the neutral kaon system was discovered in 1964 by Christenson, Cronin, Fitch, and Turlay, who observed the decay of a K_L into two pions [1]. This decay would be forbidden in the case of exact *CP* symmetry. The parameter ϵ_K measures indirect *CP* violation and is defined by

$$\epsilon_K = \frac{\mathcal{A}(K_L \to (\pi\pi)_{I=0})}{\mathcal{A}(K_S \to (\pi\pi)_{I=0})} \tag{1.1}$$

via the ratio of the respective decay amplitudes of a K_L and a K_S decaying into a two-pion state of isospin zero in such a way that direct *CP* violation is absent to a good approximation.

The parameter ϵ_K is measured with high accuracy: The value quoted by the Particle Data Group is $\epsilon_K = (2.228 \pm 0.011) \times 10^{-3} \times e^{i(43.5 \pm 0.7)^\circ}$ [2]. Whereas until about a decade ago the numerical value of ϵ_K was used as an input to determine the standard model parameters, nowadays it plays a central role in constraining models of new physics: The near diagonality of the Cabibbo-Kobayashi-Maskawa (CKM) matrix leads to a suppression in the standard model, while ϵ_K can be predicted very reliably.

For the theoretical prediction it is useful to express ϵ_K in terms of $\langle \bar{K}^0 | \mathcal{H}_{f=3}^{|\Delta S|=2} | K^0 \rangle = 2 M_K M_{12}^*$, the matrix element of the $\Delta S = 2$ effective Hamiltonian, and write

$$\epsilon_K = e^{i\phi_\epsilon} \sin\phi_\epsilon \left(\frac{\mathrm{Im}(M_{12}^*)}{\Delta M_K} + \xi \right). \tag{1.2}$$

Here M_K is the neutral kaon mass and ΔM_K the kaon mass difference, the phase of ϵ_K is $\phi_\epsilon = 43.5(7)^\circ$ [2], and $\xi = \mathrm{Im}A_0/\mathrm{Re}A_0 \simeq 0$ is the imaginary part divided by the real part of the isospin zero amplitude $A_0 = \mathcal{A}(K_S \to (\pi\pi)_{I=0})$. The ratio $\kappa_\epsilon = |\epsilon_K^{\mathrm{SM}}/\epsilon_K(\phi_\epsilon = 45^\circ, \xi = 0)|$ encompasses the change of $|\epsilon_K|$ if the values $\phi_\epsilon = 45^\circ$ and $\xi = 0$ are used in (1.2), as has been done in most of the older analyses, instead of the exact values. The authors of Ref. [3] give the value of $\kappa_\epsilon = 0.94 \pm 0.02$ in the standard model, including in their analysis also contributions of higher-dimensional operators to the absorptive and dispersive part of the K^0-$\bar{K}^0$ mixing amplitude.

The box diagram of Fig. 1(a) gives the leading contribution to the effective Hamiltonian $\mathcal{H}_{f=3}^{|\Delta S|=2}$ and the parameter M_{12}. It is proportional to a sum of loop functions times CKM factors, which, using $\lambda_i = V_{is}^* V_{id}$ and $x_i = m_i^2/M_W^2$, we can write as

$$\sum_{u_i, u_j \in \{u,c,t\}} \lambda_{u_i} \lambda_{u_j} \tilde{S}(x_{u_i}, x_{u_j}) =: \lambda_t^2 S(x_t) + \lambda_c^2 S(x_c) + 2\lambda_c \lambda_t S(x_t, x_c), \tag{1.3}$$

where $\tilde{S}$ denotes the contributions of the individual box diagrams. After the Glashow-Iliopoulos-Maiani (GIM)

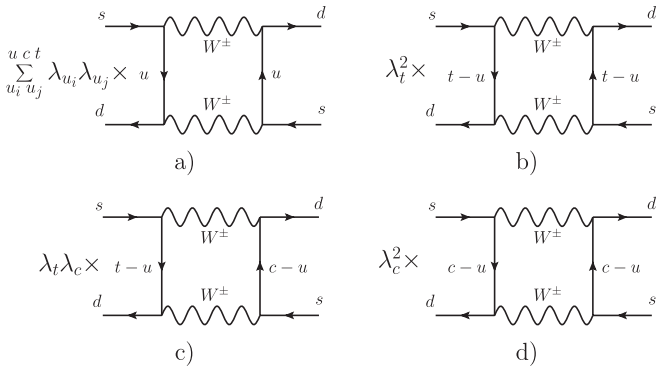

FIG. 1. The $\Delta S = 2$ box-type diagram with internal up, charm, and top contributions is expressed as a sum of box-type diagrams proportional to λ_t^2, λ_c^2, and $\lambda_t\lambda_c$, respectively, using the GIM mechanism.

mechanism has been used to eliminate $\lambda_u = -\lambda_t - \lambda_c$ it comprises the top-quark contribution—proportional to λ_t^2 [Fig. 1(b)], the charm-quark contribution—proportional to λ_c^2 [Fig. 1(c)], and the charm-top-quark contribution [Fig. 1(d)]—proportional to $\lambda_c\lambda_t$. The resulting loop functions $S(x_i, x_j) = \tilde{S}(x_i, x_j) - \tilde{S}(x_i, 0) - \tilde{S}(0, x_j) + \tilde{S}(0, 0)$ and $S(x_i) = S(x_i, x_i)$ are suppressed by the smallness of the quark mass m_i if x_i is significantly smaller than 1. This, together with the severe Cabibbo suppression of the CP violating top-quark contribution, lets all three contributions compete in size for ϵ_K:

$$\begin{aligned}&\mathrm{Im}(\lambda_t^2 S(x_t) + \lambda_c^2 S(x_c) + 2\lambda_t\lambda_c S(x_t, x_c))\\ &\quad\simeq \mathcal{O}(\lambda^{10}) + \mathcal{O}\left(\lambda^6 \frac{m_c^2}{M_W^2}\right) + \mathcal{O}\left(\lambda^6 \frac{m_c^2}{M_W^2}\log\left(\frac{m_c}{M_W}\right)\right),\end{aligned} \tag{1.4}$$

where $\lambda = |V_{us}| \approx 0.2255$. The diagram of Fig. 1(a) induces a large logarithm $\log m_c/M_W$ only for the charm-top-quark contribution: The large logarithm from the up quarks in Fig. 1(b) is power suppressed by $\Lambda_{\mathrm{QCD}}^2/M_W^2$, while the GIM mechanism cancels a potential $\log m_c/M_W$ between the diagrams with both one up and one charm quark and the diagram with only internal charm quarks.

This can be reformulated in the language of an effective theory: The dimension-six penguin as well as the current-current operators, which have tree-level Wilson coefficients, mix only into the charm-top-quark contribution, via the bilocal mixing in Fig. 2(a), yet do not induce large logarithms times tree-level Wilson coefficients proportional to λ_t^2 and λ_c^2. QCD corrections do not change this picture but only induce the well-known renormalization group effects for the $\Delta S = 1$ effective Hamiltonian [4] and for the $\Delta S = 2$ operator $\tilde{Q}_{S2}$ [Fig. 2(b)]. A leading order (LO) analysis of the charm-quark and top-quark contribution to ϵ_k then requires a one-loop calculation both for the matching at μ_W and for the running, and for the charm-quark contribution also for the matching at μ_c [Fig. 2(a)]. This is in contrast to the charm-top-quark contribution where a tree-level matching at μ_W and μ_c is sufficient at LO.

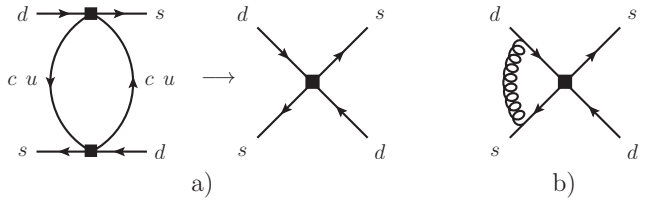

FIG. 2. Dimension-six current-current and penguin operators mix at LO into $\tilde{Q}_{S2}$ with a CKM factor $\lambda_t\lambda_c$ in (a). Integrating out the charm-quark results in similar diagrams for the LO and NLO matching of the contribution proportional to $\lambda_t\lambda_c$ and λ_c^2, respectively. A sample diagram which is relevant to the LO evolution of $\tilde{Q}_{S2}$ is shown in (b).

After integrating out the charm quark the $\Delta S = 2$ effective Hamiltonian reads

$$\begin{aligned}\mathcal{H}_{f=3}^{\Delta S=2} = \frac{G_F^2}{4\pi^2} M_W^2 [&\lambda_c^2 \eta_{cc} S(x_c) + \lambda_t^2 \eta_{tt} S(x_t) + 2\lambda_c\lambda_t \eta_{ct}\\ &\times S(x_c, x_t)] b(\mu) \tilde{Q}_{S2} + \mathrm{H.c.} + \cdots,\end{aligned} \tag{1.5}$$

where G_F is the Fermi constant and

$$\tilde{Q}_{S2} = (\bar{s}_L \gamma_\mu d_L) \otimes (\bar{s}_L \gamma^\mu d_L) \tag{1.6}$$

is the leading local four-quark operator that induces the $|\Delta S| = 2$ transition, defined in terms of the left-handed s- and d-quark fields. The QCD and logarithmic corrections are known at LO [5] and next-to-leading order (NLO) and are parametrized by $\eta_{cc} = 1.43(23)$ [6], $\eta_{ct} = 0.47(4)$[1] [7], and $\eta_{tt} = 0.5765(65)$ [8]. The parameter $b(\mu)$ is factored out such that the bag factor

$$\hat{B}_K = \frac{3}{2} b(\mu) \frac{\langle \bar{K}^0 | \tilde{Q}_{S2} | K^0 \rangle}{f_K^2 M_K^2} \tag{1.7}$$

is a renormalization-group invariant quantity, which can be calculated on the lattice with high precision—see for instance [9]. Here f_K is the kaon decay constant.

Finally note that $\mathcal{H}_{f=3}^{\Delta S=2}$ also contains higher-dimensional operators and current-current operators with up quarks, as indicated by the ellipses in Eq. (1.5). At LO in the $1/N_c$ expansion (N_c being the number of colors) only one higher-dimensional operator is present and its matrix element is estimated in [3,10] to result in a 0.5% enhancement of ϵ_K.

In view of the improvements on the long-distance corrections achieved in recent years, the short-distance contributions should be reconsidered. In this work we calculate the next-to-next-to-leading order (NNLO) corrections to the charm-top contribution η_{ct}. The NNLO corrections to the charm-quark contribution η_{cc} will be presented in a forthcoming publication [11].

This paper is organized as follows. In Sec. II we define the effective Hamiltonian relevant to $\Delta S = 2$ transitions. We present the details of our calculation as well as the analytic results in Sec. III. The discussion and numerical evaluation follow in Sec. IV. In the Appendix we show how our results transform under a change of the operator basis.

II. EFFECTIVE HAMILTONIAN FOR NEUTRAL KAON MIXING

The effective Hamiltonian $\mathcal{H}_{f=3}^{\Delta S=2}$ of Eq. (1.5) describes the dominant contribution to $\Delta S = 2$ processes below the charm-quark mass scale. The loop functions

$$S(x_c) = x_c + \mathcal{O}(x_c^2), \tag{2.1}$$

[1]Our analysis, which uses different inputs for the physical parameters and a different error estimate, yields a NLO value of $\eta_{ct} = 0.457(73)$; see Section IV.

$$S(x_t) = \frac{4x_t - 11x_t^2 + x_t^3}{4(1-x_t)^2} - \frac{3x_t^3 \log x_t}{2(1-x_t)^3}, \tag{2.2}$$

$$S(x_c, x_t) = -x_c \log x_c + x_c F(x_t) + \mathcal{O}(x_c^2 \log x_c), \tag{2.3}$$

where the function F is defined as

$$F(x_t) = \frac{x_t^2 - 8x_t + 4}{4(1-x_t)^2} \log x_t - \frac{3x_t}{4(1-x_t)}, \tag{2.4}$$

are used as normalization factors of the three contributions proportional to λ_c^2, λ_t^2, and $\lambda_c\lambda_t$ in Eq. (1.5). In this normalization we fix the charm-quark mass and the top-quark mass to $m_c = m_c^{\overline{\rm MS}}(m_c)$ and $m_t = m_t^{\overline{\rm MS}}(m_t)$, respectively, in x_c and x_t. This avoids spurious scale dependences in η_{ct}, η_{cc}, and η_{tt}, if these parameters are defined through Eq. (1.5).[2]

A. The operator basis

Above the charm-quark mass scale both the $\Delta S = 1$ and $\Delta S = 2$ effective Hamiltonians contribute to the Wilson coefficient of $\tilde{Q}_{S2}$ through renormalization group effects. In the following we list all operators needed for these effective Hamiltonians. They can be divided into three classes: Physical operators, gauge-invariant operators that vanish by the QCD equations of motion (EOM), and evanescent operators, that vanish algebraically in four space-time dimensions.

We start with the dimension-six operators, which we choose such that problems arising from the γ_5 matrix appearing in closed fermion loops in the framework of dimensional regularization do not occur [12]. There are two current-current operators

$$\begin{aligned} Q_1^{qq'} &= (\bar{s}_L \gamma_\mu T^a q_L) \otimes (\bar{q}'_L \gamma^\mu T^a d_L), \\ Q_2^{qq'} &= (\bar{s}_L \gamma_\mu q_L) \otimes (\bar{q}'_L \gamma^\mu d_L), \end{aligned} \tag{2.5}$$

where $q_L = \frac{1}{2}(1-\gamma_5)q$ is the left-handed chiral quark field, and q and q' are either u or c. The color matrices T^a are normalized such that $\mathrm{Tr} T^a T^b = \delta^{ab}/2$. We use these operators in the linear combination

$$\begin{aligned} Q_\pm^{qq'} &= \frac{1}{2}\left(1 \pm \frac{1}{N_c}\right) Q_2^{qq'} \pm Q_1^{qq'} \\ &= \frac{1}{2}((\bar{s}_L^\alpha \gamma_\mu q_L^\alpha) \otimes (\bar{q}_L'^\beta \gamma^\mu d_L^\beta) \\ &\quad \pm (\bar{s}_L^\alpha \gamma_\mu q_L^\beta) \otimes (\bar{q}_L'^\beta \gamma^\mu d_L^\alpha)), \end{aligned} \tag{2.6}$$

where α and β are color indices, and N_c is the number of colors. The advantage is that the anomalous dimensions in the subspace of current-current operators are diagonal in this basis.[3]

[2]The parameters η_{cc}, η_{tt}, and η_{ct} equal η_1^*, η_2^*, and η_3^*, respectively, as defined in Ref. [7].

[3]This is true beyond LO only with a suitable choice of the evanescent operators; see below.

We define the QCD penguin operators as

$$\begin{aligned} Q_3 &= (\bar{s}_L \gamma_\mu d_L) \otimes \sum_q (\bar{q} \gamma^\mu q), \\ Q_4 &= (\bar{s}_L \gamma_\mu T^a d_L) \otimes \sum_q (\bar{q} \gamma^\mu T^a q), \\ Q_5 &= (\bar{s}_L \gamma_{\mu_1\mu_2\mu_3} d_L) \otimes \sum_q (\bar{q} \gamma^{\mu_1\mu_2\mu_3} q), \\ Q_6 &= (\bar{s}_L \gamma_{\mu_1\mu_2\mu_3} T^a d_L) \otimes \sum_q (\bar{q} \gamma^{\mu_1\mu_2\mu_3} T^a q), \end{aligned} \tag{2.7}$$

where the sum extends over the light-quark fields, and we have introduced the abbreviations $\gamma_{\mu_1\mu_2\mu_3} = \gamma_{\mu_1}\gamma_{\mu_2}\gamma_{\mu_3}$, etc.

In order to subtract the divergences of all possible one-particle irreducible (1PI) subdiagrams of the relevant Green's functions, we need the following gauge-invariant EOM-vanishing operator:

$$Q_{\rm EOM} = \frac{1}{g} \bar{s}_L \gamma^\mu T^a d_L D^\nu G^a_{\mu\nu} + Q_4, \tag{2.8}$$

where D_μ denotes the covariant derivative, acting on the gluon field, and $g^2 = 4\pi\alpha_s$ is the square of the strong coupling constant. Sample diagrams are shown in Fig. 3.

The operator inducing the effective $|\Delta S| = 2$ interactions above the charm-quark scale can be chosen as

$$\tilde{Q}_7 = \frac{m_c^2}{g^2 \mu^{2\epsilon}} (\bar{s}_L^\alpha \gamma_\mu d_L^\alpha) \otimes (\bar{s}_L^\beta \gamma^\mu d_L^\beta), \tag{2.9}$$

where α and β again denote color indices: Note that, according to convention, we define the operator with two inverse powers of the strong coupling constant in order to account for the logarithm already present at leading order.

The use of dimensional regularization in a theory involving fermions implies an infinite-dimensional Dirac algebra. In order to remove all divergences of the Green's functions, we have to introduce a set of evanescent operators that are nonzero in d dimensions and vanish algebraically in four dimensions. At the one-loop level we need

$$\begin{aligned} E_1^{qq'(1)} &= (\bar{s}_L \gamma_{\mu_1\mu_2\mu_3} T^a q_L) \otimes (\bar{q}'_L \gamma^{\mu_1\mu_2\mu_3} T^a d_L) \\ &\quad - (16 - 4\epsilon - 4\epsilon^2) Q_1^{qq'}, \\ E_2^{qq'(1)} &= (\bar{s}_L \gamma_{\mu_1\mu_2\mu_3} q_L) \otimes (\bar{q}'_L \gamma^{\mu_1\mu_2\mu_3} d_L) \\ &\quad - (16 - 4\epsilon - 4\epsilon^2) Q_2^{qq'}, \\ E_3^{(1)} &= (\bar{s}_L \gamma_{\mu_1\mu_2\mu_3\mu_4\mu_5} d_L) \otimes \sum_q (\bar{q} \gamma^{\mu_1\mu_2\mu_3\mu_4\mu_5} q) \\ &\quad + 64 Q_3 - 20 Q_5, \\ E_4^{(1)} &= (\bar{s}_L \gamma_{\mu_1\mu_2\mu_3\mu_4\mu_5} T^a d_L) \otimes \sum_q (\bar{q} \gamma^{\mu_1\mu_2\mu_3\mu_4\mu_5} T^a q) \\ &\quad + 64 Q_4 - 20 Q_6. \end{aligned} \tag{2.10}$$

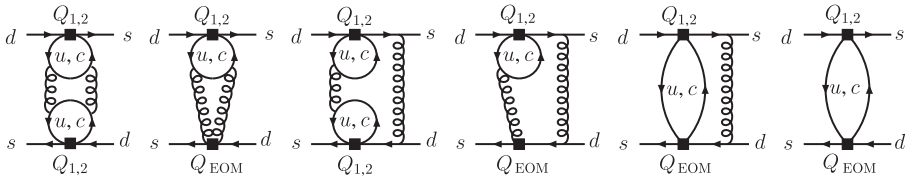

FIG. 3. Sample three-loop diagrams with 1PI subdivergences that have to be subtracted by insertions of the EOM-vanishing operator. The corresponding 1PI one- and two-loop insertions of $Q_{\rm EOM}$ are also shown.

At the two-loop level, we use the following four operators:

$$
\begin{aligned}
E_1^{qq'(2)} &= (\bar{s}_L\gamma_{\mu_1\mu_2\mu_3\mu_4\mu_5}T^a q_L)\otimes(\bar{q}'_L\gamma^{\mu_1\mu_2\mu_3\mu_4\mu_5}T^a d_L) - \left(256 - 224\epsilon - \frac{5712}{25}\epsilon^2\right)Q_1^{qq'},\\
E_2^{qq'(2)} &= (\bar{s}_L\gamma_{\mu_1\mu_2\mu_3\mu_4\mu_5}q_L)\otimes(\bar{q}'_L\gamma^{\mu_1\mu_2\mu_3\mu_4\mu_5}d_L) - \left(256 - 224\epsilon - \frac{10032}{25}\epsilon^2\right)Q_2^{qq'},\\
E_3^{(2)} &= (\bar{s}_L\gamma_{\mu_1\mu_2\mu_3\mu_4\mu_5\mu_6\mu_7}d_L)\otimes\sum_q(\bar{q}\gamma^{\mu_1\mu_2\mu_3\mu_4\mu_5\mu_6\mu_7}q) + 1280Q_3 - 336Q_5,\\
E_4^{(2)} &= (\bar{s}_L\gamma_{\mu_1\mu_2\mu_3\mu_4\mu_5\mu_6\mu_7}T^a d_L)\otimes\sum_q(\bar{q}\gamma^{\mu_1\mu_2\mu_3\mu_4\mu_5\mu_6\mu_7}T^a q) + 1280Q_4 - 336Q_6.
\end{aligned}
\tag{2.11}
$$

The evanescent operators in the current-current sector are chosen such that the anomalous dimensions for the operators $Q_\pm^{qq'}$ are diagonal through NNLO [13]. The remaining operators are chosen as in Ref. [12].

In addition to the operator $\tilde{Q}_7$ with the color structure $(\bar{s}_L^\alpha\gamma_\mu d_L^\alpha)\otimes(\bar{s}_L^\beta\gamma^\mu d_L^\beta)$, the dimension-six and dimension-eight operators will also mix into an operator with the color structure $(\bar{s}_L^\alpha\gamma_\mu d_L^\beta)\otimes(\bar{s}_L^\beta\gamma^\mu d_L^\alpha)$. In four space-time dimensions, the latter is related to the former structure by a Fierz transformation. The difference of these structures is therefore evanescent, and correspondingly we introduce an evanescent operator of the following form:

$$
\tilde{E}_F = \frac{m_c^2}{g^2\mu^{2\epsilon}}(\bar{s}_L^\alpha\gamma_\mu d_L^\beta)\otimes(\bar{s}_L^\beta\gamma^\mu d_L^\alpha) - \tilde{Q}_7. \tag{2.12}
$$

We choose the remaining evanescent dimension-eight operators to be

$$
\begin{aligned}
\tilde{E}_7^{(1)} &= \frac{m_c^2}{g^2\mu^{2\epsilon}}\left(\bar{s}_L^\alpha\gamma_{\mu_1\mu_2\mu_3}d_L^\alpha\right)\otimes\left(\bar{s}_L^\beta\gamma^{\mu_1\mu_2\mu_3}d_L^\beta\right) - (16 - 4\epsilon - 4\epsilon^2)\tilde{Q}_7,\\
\tilde{E}_8^{(1)} &= \frac{m_c^2}{g^2\mu^{2\epsilon}}\left(\bar{s}_L^\alpha\gamma_{\mu_1\mu_2\mu_3}d_L^\beta\right)\otimes\left(\bar{s}_L^\beta\gamma^{\mu_1\mu_2\mu_3}d_L^\alpha\right) - (16 - 4\epsilon - 4\epsilon^2)(\tilde{Q}_7 + \tilde{E}_F),\\
\tilde{E}_7^{(2)} &= \frac{m_c^2}{g^2\mu^{2\epsilon}}\left(\bar{s}_L^\alpha\gamma_{\mu_1\mu_2\mu_3\mu_4\mu_5}d_L^\alpha\right)\otimes\left(\bar{s}_L^\beta\gamma^{\mu_1\mu_2\mu_3\mu_4\mu_5}d_L^\beta\right) - \left(256 - 224\epsilon - \frac{108816}{325}\epsilon^2\right)\tilde{Q}_7,\\
\tilde{E}_8^{(2)} &= \frac{m_c^2}{g^2\mu^{2\epsilon}}\left(\bar{s}_L^\alpha\gamma_{\mu_1\mu_2\mu_3\mu_4\mu_5}d_L^\beta\right)\otimes\left(\bar{s}_L^\beta\gamma^{\mu_1\mu_2\mu_3\mu_4\mu_5}d_L^\alpha\right) - \left(256 - 224\epsilon - \frac{108816}{325}\epsilon^2\right)(\tilde{Q}_7 + \tilde{E}_F),\\
\tilde{E}_7^{(3)} &= \frac{m_c^2}{g^2\mu^{2\epsilon}}\left(\bar{s}_L^\alpha\gamma_{\mu_1\mu_2\mu_3\mu_4\mu_5\mu_6\mu_7}d_L^\alpha\right)\otimes\left(\bar{s}_L^\beta\gamma^{\mu_1\mu_2\mu_3\mu_4\mu_5\mu_6\mu_7}d_L^\beta\right) - 4096\tilde{Q}_7,\\
\tilde{E}_8^{(3)} &= \frac{m_c^2}{g^2\mu^{2\epsilon}}\left(\bar{s}_L^\alpha\gamma_{\mu_1\mu_2\mu_3\mu_4\mu_5\mu_6\mu_7}d_L^\beta\right)\otimes\left(\bar{s}_L^\beta\gamma^{\mu_1\mu_2\mu_3\mu_4\mu_5\mu_6\mu_7}d_L^\alpha\right) - 4096(\tilde{Q}_7 + \tilde{E}_F).
\end{aligned}
\tag{2.13}
$$

This choice ensures that $\tilde{Q}_{S2}$ will have the same anomalous dimension as Q_+ up to NNLO. It is given explicitly here for the first time.

B. Effective Hamiltonian

We obtain the effective Hamiltonian valid between the electroweak and the bottom-quark scale by removing the

top quark and the W boson as dynamical degrees of freedom from the standard model. It reads in terms of the renormalized Wilson coefficients

$$\mathcal{H}_{f=5}^{\text{eff}} = \frac{4G_F}{\sqrt{2}} \sum_{i=+,-,3}^{6} C_i \Bigg[\sum_{j=+,-} Z_{ij} \sum_{k,l=u,c} V_{ks}^* V_{ld} Q_j^{kl} - \lambda_t \sum_{j=3}^{6} Z_{ij} Q_j \Bigg] + \frac{G_F^2}{4\pi^2} \lambda_t^2 \tilde{C}_{S2}^t \tilde{Z}_{S2} \tilde{Q}_{S2} + 8 G_F^2 \lambda_c \lambda_t \times \Bigg[\sum_{k=+,-} \sum_{l=+,-,3}^{6} C_k C_l \hat{Z}_{kl,7} + \tilde{C}_7 \tilde{Z}_{77} \Bigg] \tilde{Q}_7 + \text{H.c.} \tag{2.14}$$

Here the term in the first square brackets represents the $|\Delta S| = 1$ part of the effective Hamiltonian, whereas the remaining terms constitute the $|\Delta S| = 2$ contributions. The first term of the latter is related to a single insertion of $\tilde{Q}_{S2}$, induced by the top-quark contribution to the standard model amplitude. The remaining terms arise from the mixing of insertions of two $|\Delta S| = 1$ operators into the operator $\tilde{Q}_7$. The GIM mechanism leads to the absence of a λ_c^2 contribution to the Wilson coefficient of $\tilde{Q}_7$. The renormalization constants Z are defined such that any renormalized effective amplitude, of the form

$$\mathcal{A}_{\text{eff}} = C_i(\mu) Z_{ij} \langle Z Q_j \rangle_R + (C_k C_{k'} \hat{Z}_{kk',l} + \tilde{C}_k \tilde{Z}_{kl}) \langle Z \tilde{Q}_l \rangle_R,$$

is finite and implicitly includes the contribution of evanescent operators. Here angle-brackets denote matrix elements between initial and final states i and f, respectively, i.e. $\langle Q_j \rangle = \langle f | Q_j | i \rangle$. Z denotes the wave function renormalization of the fields in the operator, so that $\langle Z Q_i \rangle_R$ are the renormalized matrix elements of the bare operator Q_i^{bare}, where masses and gauge couplings are renormalized in the usual way.

The effective Hamiltonian $\mathcal{H}_{f=4}^{\text{eff}}$ valid between the bottom- and the charm-quark scale looks exactly the same as $\mathcal{H}_{f=5}^{\text{eff}}$. The only difference is induced by the presence of penguin operators, which explicitly depend on all light-quark fields.

Below the charm-quark scale, the charm quark is removed as a dynamical degree of freedom. As a consequence, the $|\Delta S| = 1$ operators can now be dropped from the effective Lagrangian, because the matrix elements of double insertions of these operators are suppressed by factors of m_s^2/M_W^2. The effective Hamiltonian is thus given by

$$\mathcal{H}_{f=3}^{|\Delta S|=2} = \frac{G_F^2}{4\pi^2} [\lambda_c^2 \tilde{C}_{S2}^c(\mu) + \lambda_t^2 \tilde{C}_{S2}^t(\mu) + \lambda_c \lambda_t \tilde{C}_{S2}^{ct}(\mu)] \tilde{Z}_{S2} \tilde{Q}_{S2} \tag{2.15}$$

and now only contains the $|\Delta S| = 2$ operator $\tilde{Q}_{S2}$ defined in Eq. (1.6).

III. CALCULATION OF η_{ct}

In this section we present the details of the calculation of η_{ct} in the NNLO approximation. We start with the determination of the initial conditions for the Wilson coefficients at the electroweak scale. Afterward we use the renormalization group equations to evolve them down to the charm-quark scale, including the threshold corrections at the bottom-quark scale. Finally we determine the charm-top contribution to $\tilde{C}_{S2}^{ct}$ by a matching calculation at the charm-quark scale.

A. Initial conditions at the electroweak scale

The initial conditions for the Wilson coefficients of the dimension-six operators are available in the literature. In our basis, where we can use a naive anticommuting γ_5, the results up to second order in $\alpha_s^{(f=5)}$ read[4]

$$\begin{aligned}
C_\pm(\mu) &= 1 \pm \frac{1}{2}\left(1 \mp \frac{1}{3}\right)(11 + 6L_W)\frac{\alpha_s^{(5)}(\mu)}{4\pi} + \left(\frac{1}{18}(7 \pm 51)\pi^2 \mp \frac{1}{2}\left(1 \mp \frac{1}{3}\right)T(x_t) - \frac{1}{3600}(135677 \mp 124095)\right. \\
&\quad \left. - \frac{5}{36}(11 \mp 249)L_W + \frac{1}{6}(7 \pm 51)L_W^2\right)\left(\frac{\alpha_s^{(5)}(\mu)}{4\pi}\right)^2, \\
C_3(\mu) &= \left(\frac{\alpha_s^{(5)}(\mu)}{4\pi}\right)^2\left(G_1^t(x_t) - \frac{680}{243} - \frac{20}{81}\pi^2 - \frac{68}{81}L_W - \frac{20}{27}L_W^2\right), \\
C_4(\mu) &= \frac{\alpha_s^{(5)}(\mu)}{4\pi}\left(E_0^t(x_t) - \frac{7}{9} + \frac{2}{3}L_W\right) + \left(\frac{\alpha_s^{(5)}(\mu)}{4\pi}\right)^2\left(E_1^t(x_t) + \frac{842}{243} + \frac{10}{81}\pi^2 + \frac{124}{27}L_W + \frac{10}{27}L_W^2\right), \\
C_5(\mu) &= \left(\frac{\alpha_s^{(5)}(\mu)}{4\pi}\right)^2\left(\frac{2}{15}E_0^t(x_t) - \frac{1}{10}G_1^t(x_t) + \frac{68}{243} + \frac{2}{81}\pi^2 + \frac{14}{81}L_W + \frac{2}{27}L_W^2\right), \\
C_6(\mu) &= \left(\frac{\alpha_s^{(5)}(\mu)}{4\pi}\right)^2\left(\frac{1}{4}E_0^t(x_t) - \frac{3}{16}G_1^t(x_t) + \frac{85}{162} + \frac{5}{108}\pi^2 + \frac{35}{108}L_W + \frac{5}{36}L_W^2\right).
\end{aligned} \tag{3.1}$$

We have taken the initial conditions for $C_\pm$ from Ref. [13]. The initial conditions for $C_3 \ldots C_6$ can be found in

[4]Here and in the following, by the superscript in brackets we display explicitly the number of light-quark flavors for which α_s is defined.

Ref. [14], where also the loop functions $T(x_t)$, $G_1^t(x_t)$, $E_0^t(x_t)$, and $E_1^t(x_t)$ are defined. Note that in our renormalization scheme we had to include an additional finite contribution for C_4, as described in the Appendix. We have introduced the abbreviation $L_W = \log(\mu^2/M_W^2)$.

With these ingredients, we can now calculate the initial conditions for the Wilson coefficients of the dimension-eight operators. In order to match the Green's functions in the standard model and the effective five-flavor theory, we have to compute the finite parts of Feynman diagrams of the type shown in Figs. 1 and 4. To this end, we perform a Taylor expansion in the charm-quark mass of all propagators corresponding to a charm-quark field. The constant terms cancel because of the GIM mechanism, whereas the terms proportional to m_c^2 give the leading nonvanishing contribution we are interested in. This procedure leads to massless vacuum integrals in the effective theory, such that only terms proportional to tree-level matrix elements remain. Some of these terms multiply divergent renormalization constants and correspond to infrared divergences in the effective theory. They exactly cancel the corresponding infrared divergent terms in the standard model, leaving us with a finite result.

Expanding the dimension-eight Wilson coefficient as

$$\tilde{C}_7(\mu) = \tilde{C}_7^{(0)}(\mu) + \frac{\alpha_s^{(5)}(\mu)}{4\pi}\tilde{C}_7^{(1)}(\mu) + \left(\frac{\alpha_s^{(5)}(\mu)}{4\pi}\right)^2 \tilde{C}_7^{(2)}(\mu), \tag{3.2}$$

we obtain the following result:

$$\begin{aligned}
\tilde{C}_7^{(0)}(\mu) &= 0, \qquad \tilde{C}_7^{(1)}(\mu) = F(x_t) + \frac{1}{2} - L_W, \\
\tilde{C}_7^{(2)}(\mu) &= +\frac{5x_t^3 - 21x_t^2 + 60x_t - 20}{2(x_t-1)^3}\log(x_t)L_W + \frac{12x_t^5 - 34x_t^4 - 9x_t^3 - 33x_t^2 - 116x_t + 36}{12(x_t-1)^3}\log^2(x_t) \\
&\quad + \frac{-12x_t^5 + 27x_t^4 + 23x_t^3 + 150x_t^2 - 108x_t + 16}{6(x_t-1)^3 x_t}\log(x_t) \\
&\quad + \frac{-7800x_t^4 - 126499x_t^3 + 191248x_t^2 - 129749x_t + 10400}{3900(x_t-1)^2 x_t} \\
&\quad + \frac{6x_t^6 - 11x_t^5 - 8x_t^4 - 29x_t^3 + 23x_t^2 - 16x_t + 8}{3(x_t-1)^2 x_t^2}\mathrm{Li}_2(1-x_t) \\
&\quad + \frac{6x_t^4 + x_t^3 - 59x_t^2 - 8}{3x_t^2}\zeta_2 - \frac{47x_t^2 - 31x_t + 56}{6(x_t-1)^2}L_W - 7L_W^2
\end{aligned} \tag{3.3}$$

The first line in Eq. (3.3) agrees with the result obtained already by Herrlich and Nierste in [7] after the corresponding change of the renormalization scheme. The two-loop result is new.

B. Structure of the renormalization group equations

After the determination of the initial conditions for the Wilson coefficients, the next step is the renormalization group evolution to lower scales. The renormalization group equation relevant for the Wilson coefficient $\tilde{C}_7$ is given by

$$\mu\frac{d}{d\mu}\tilde{C}_7(\mu) = \tilde{C}_7(\mu)\tilde{\gamma}_{77} + \sum_{k=+,-}\sum_{n=+,-,3}^{6} C_k(\mu)C_n(\mu)\hat{\gamma}_{kn,7}, \tag{3.4}$$

where $\tilde{\gamma}_{77}$ denotes the anomalous dimension matrix of the operator $\tilde{Q}_7$, and $\hat{\gamma}_{kn,7}$ is the anomalous dimension tensor, describing the mixing of the dimension-six operators into $\tilde{Q}_7$. The matrix $\tilde{\gamma}_{77}$ is decomposed as $\tilde{\gamma}_{77} = \tilde{\gamma}_{S2} + 2\gamma_m - 2\beta$, where the anomalous dimension of the quark mass γ_m and the β function are related to the factor m_c^2/g^2

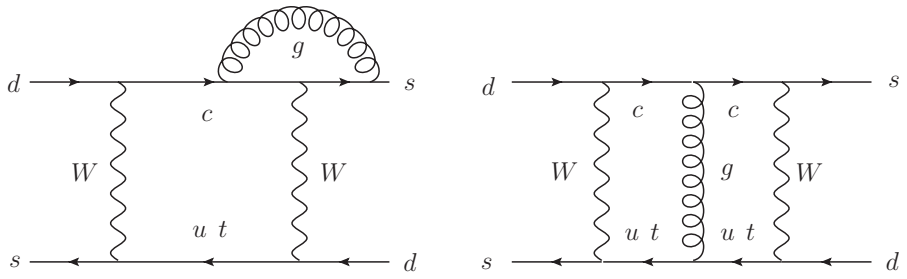

FIG. 4. Sample two-loop Feynman diagrams contributing to the matching at the electroweak scale.

in the definition of the operator $\tilde{Q}_7$. The anomalous dimension matrix $\tilde{\gamma}_{S2}$ is defined in terms of the renormalization constants $\tilde{Z}_{S2}$ as

$$\tilde{\gamma}_{S2} = \tilde{Z}_{S2}\mu\frac{d}{d\mu}\tilde{Z}_{S2}^{-1}. \tag{3.5}$$

The explicit expressions for the anomalous dimension matrix in terms of the renormalization constants $\tilde{Z}_{S2}$ are given up to NNLO by

$$\begin{aligned}
\tilde{\gamma}_{S2}^{(0)} &= 2\tilde{Z}_{S2}^{(1,1)},\\
\tilde{\gamma}_{S2}^{(1)} &= 4\tilde{Z}_{S2}^{(2,1)} - 2\tilde{Z}_{S2}^{(1,1)}\tilde{Z}_{S2}^{(1,0)},\\
\tilde{\gamma}_{S2}^{(2)} &= 6\tilde{Z}_{S2}^{(3,1)} - 4\tilde{Z}_{S2}^{(2,1)}\tilde{Z}_{S2}^{(1,0)} - 2\tilde{Z}_{S2}^{(1,1)}\tilde{Z}_{S2}^{(2,0)},
\end{aligned} \tag{3.6}$$

where we only kept the nonvanishing physical contributions. Here the superscript (n, m) denotes the $1/\epsilon^m$-pole part of the n-loop contribution. The anomalous dimension tensor is defined as [15]

$$\begin{aligned}
\hat{\gamma}_{kn,l} = &-(\gamma_{kk'}\delta_{nn'} + \gamma_{nn'}\delta_{kk'})\hat{Z}_{k'n',l'}\tilde{Z}_{l'l}^{-1}\\
&-\left(\mu\frac{d}{d\mu}\hat{Z}_{kn,l'}\right)\tilde{Z}_{l'l}^{-1}.
\end{aligned} \tag{3.7}$$

The nonvanishing contributions to the physical part of the anomalous dimension tensor are given in terms of the renormalization constants by

$$\begin{aligned}
\hat{\gamma}_{kn,l}^{(0)} &= 2\hat{Z}_{kn,l}^{(1,1)},\\
\hat{\gamma}_{kn,l}^{(1)} &= 4\hat{Z}_{kn,l}^{(2,1)} - 2\hat{Z}_{kn,l'}^{(1,1)}\tilde{Z}_{l'l}^{(1,0)}\\
&\quad - 2\left\{Z_{kk'}^{(1,1)}\delta_{nn'} + \delta_{kk'}Z_{nn'}^{(1,1)}\right\}\hat{Z}_{k'n',l}^{(1,0)},\\
\hat{\gamma}_{kn,l}^{(2)} &= 6\hat{Z}_{kn,l}^{(3,1)} - 4\hat{Z}_{kn,l'}^{(2,1)}\tilde{Z}_{l'l}^{(1,0)} - 2\hat{Z}_{kn,l'}^{(1,1)}\tilde{Z}_{l'l}^{(2,0)}\\
&\quad - 2\left\{Z_{kk'}^{(1,1)}\delta_{nn'} + \delta_{kk'}Z_{nn'}^{(1,1)}\right\}\hat{Z}_{k'n',l}^{(2,0)}\\
&\quad - 4\left\{Z_{kk'}^{(2,1)}\delta_{nn'} + \delta_{kk'}Z_{nn'}^{(2,1)}\right\}\hat{Z}_{k'n',l}^{(1,0)},
\end{aligned} \tag{3.8}$$

where the indices k, n, and l correspond to physical operators only.

In order to determine the renormalization constants, we have to compute the divergent parts of Feynman diagrams with up to three loops; see Fig. 5. We use the method suggested in [16] by Chetyrkin, Misiak, and Münz for extracting the UV divergences of a given Feynman diagram. The renormalization constants are then determined recursively by subtracting subdivergences according to Zimmermann's forest formula. As usual, we perform a finite renormalization in order to ensure the vanishing of matrix elements of evanescent operators. An additional subtlety arises because of the presence of EOM-vanishing operators at second order in the effective interactions: As explained in detail in Ref. [17], we have to expect nontrivial contact terms resulting from double insertions of Q_{EOM} and physical operators. We computed these terms explicitly, showing that nonzero contributions indeed occur, and subtracted them by an additional finite counterterm:

$$\hat{Z}^{(2,0)}_{Q_+Q_{\mathrm{EOM}},\tilde{Q}_7} = \hat{Z}^{(2,0)}_{Q_-Q_{\mathrm{EOM}},\tilde{Q}_7} = \frac{3}{8}\left(N_c - 1 - \frac{1}{N_c} - \frac{1}{N_c^2}\right). \tag{3.9}$$

This renormalization ensures the validity of the equations of motion also at second order in the effective interactions.

Let us now look at Eqs. (3.4) in more detail. It turns out that these equations are equivalent to the following system of eight equations [7]

$$\mu\frac{d}{d\mu}D = \gamma^T D, \tag{3.10}$$

where the anomalous dimension matrix and the Wilson coefficients are now given by

$$\begin{aligned}
\gamma^T &= \begin{pmatrix} \gamma_Q^T & 0 & 0\\ \tilde{\gamma}_{+,7}^T & \tilde{\gamma}_{77} - \gamma_+ & 0\\ \tilde{\gamma}_{-,7}^T & 0 & \tilde{\gamma}_{77} - \gamma_- \end{pmatrix},\\
D(\mu) &= \begin{pmatrix} C(\mu)\\ \tilde{C}_7^+(\mu)/C_+(\mu)\\ \tilde{C}_7^-(\mu)/C_-(\mu) \end{pmatrix},
\end{aligned} \tag{3.11}$$

if we decompose the Wilson coefficient $\tilde{C}_7$ as

$$\tilde{C}_7(\mu) = \tilde{C}_7^+(\mu) + \tilde{C}_7^-(\mu). \tag{3.12}$$

This decomposition is completely arbitrary and preserved by the renormalization group evolution. For instance, we may choose $\tilde{C}_7^+(\mu) = \tilde{C}_7(\mu)$ and $\tilde{C}_7^-(\mu) = 0$. The

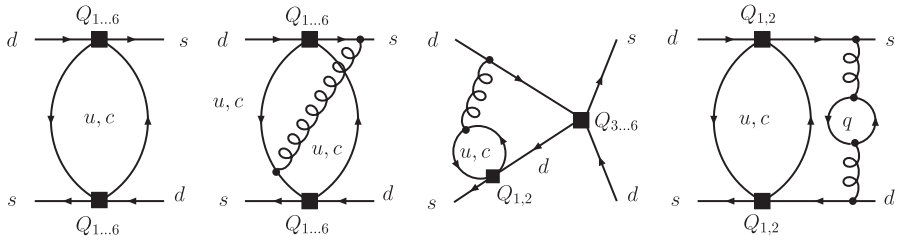

FIG. 5. Sample one-, two-, and three-loop diagrams contributing to the NNLO mixing of dimension-six into dimension-eight operators.

advantage of (3.10) is that it has the form of a renormalization group equation for a single operator insertion, and we can use the well-known explicit solution (see, for instance, Ref. [4]).

We obtain the anomalous dimension matrix γ_Q of the operators $Q_+, Q_-, Q_3, \ldots, Q_6$ from Ref. [4] by the basis transformation described in the Appendix and find

$$\gamma_Q^{(0)} = \begin{pmatrix} 4 & 0 & 0 & \frac{2}{3} & 0 & 0 \\ 0 & -8 & 0 & \frac{2}{3} & 0 & 0 \\ 0 & 0 & 0 & -\frac{52}{3} & 0 & 2 \\ 0 & 0 & -\frac{40}{9} & \frac{4}{3}f - \frac{160}{9} & \frac{4}{9} & \frac{5}{6} \\ 0 & 0 & 0 & -\frac{256}{3} & 0 & 20 \\ 0 & 0 & -\frac{256}{9} & \frac{40}{3}f - \frac{544}{9} & \frac{40}{9} & -\frac{2}{3} \end{pmatrix}, \tag{3.13}$$

$$\gamma_Q^{(1)} = \begin{pmatrix} \frac{4}{9}f - 7 & 0 & -\frac{748}{81} & \frac{415}{81} & \frac{82}{81} & \frac{35}{54} \\ 0 & -\frac{8}{9}f - 14 & \frac{332}{81} & \frac{793}{81} & -\frac{26}{81} & \frac{35}{54} \\ 0 & 0 & -\frac{4468}{81} & -\frac{52}{9}f - \frac{29129}{81} & \frac{400}{81} & \frac{3493}{108} - \frac{2}{9}f \\ 0 & 0 & \frac{368}{81}f - \frac{13678}{243} & \frac{1334}{81}f - \frac{79409}{243} & \frac{509}{486} - \frac{8}{81}f & \frac{13499}{648} - \frac{5}{27}f \\ 0 & 0 & -\frac{160}{9}f - \frac{244480}{81} & -\frac{2200}{9}f - \frac{29648}{81} & \frac{16\mathrm{Nf}}{9} + \frac{23116}{81} & \frac{148}{9}f + \frac{3886}{27} \\ 0 & 0 & \frac{77600}{243} - \frac{1264}{81}f & \frac{164}{81}f - \frac{28808}{243} & \frac{400}{81}f - \frac{20324}{243} & \frac{622}{27}f - \frac{21211}{162} \end{pmatrix}, \tag{3.14}$$

$$\gamma_Q^{(2)} = \begin{pmatrix} \frac{275267}{150} - \frac{260}{81}f^2 - \frac{52891}{675}f - \left(\frac{160}{3}f + 672\right)\zeta_3 & 0 \\ 0 & \frac{12297}{25} + \frac{520}{81}f^2 - \frac{62686}{675}f + \left(\frac{320}{3}f + 672\right)\zeta_3 \\ 0 & 0 \\ 0 & 0 \\ 0 & 0 \\ 0 & 0 \end{pmatrix}$$

$$\begin{pmatrix} \frac{54821}{4374} - \frac{160}{243}f + \frac{1360}{27}\zeta_3 & -\frac{8226427}{109350} - \frac{18845}{1458}f - \frac{2104}{27}\zeta_3 \\ \frac{1064}{243}f + \frac{1360}{27}\zeta_3 - \frac{25531}{4374} & -\frac{26513}{1458}f - \frac{664}{27}\zeta_3 + \frac{57546991}{218700} \\ \frac{14012}{243}f - \frac{608}{27}\zeta_3 - \frac{4203068}{2187} & \frac{272}{27}f^2 + \frac{888605}{2916}f + \left(160f + \frac{39824}{27}\right)\zeta_3 - \frac{18422762}{2187} \\ \frac{472}{81}f^2 + \frac{217892}{2187}f + \left(\frac{1360}{9}f + \frac{27520}{81}\right)\zeta_3 - \frac{5875184}{6561} & -\frac{4010}{729}f^2 + \frac{8860733}{17496}f + \left(\frac{2512}{27}f + \frac{16592}{81}\right)\zeta_3 - \frac{70274587}{13122} \\ -\frac{2144}{81}f^2 + \frac{358672}{81}f + \frac{87040}{27}\zeta_3 - \frac{194951552}{2187} & \frac{3088}{27}f - \frac{2949616}{729}f + \left(640f + \frac{238016}{27}\right)\zeta_3 - \frac{130500332}{2187} \\ \frac{17920}{243}f^2 - \frac{2535466}{2187}f + \left(\frac{12160}{9}f + \frac{174208}{81}\right)\zeta_3 + \frac{162733912}{6561} & -\frac{159548}{729}f^2 - \frac{1826023}{4374}f - \left(\frac{9440}{27}f + \frac{24832}{81}\right)\zeta_3 + \frac{13286236}{6561} \end{pmatrix}$$

$$\begin{pmatrix} \frac{112}{243}f - \frac{124}{27}\zeta_3 - \frac{113417}{17496} & -\frac{35}{324}f - \frac{40}{9}\zeta_3 + \frac{479581}{23328} \\ -\frac{140}{243}f - \frac{124}{27}\zeta_3 + \frac{79687}{17496} & -\frac{35}{324}f - \frac{70}{9}\zeta_3 + \frac{242737}{23328} \\ -\frac{1352}{243}f - \frac{496}{27}\zeta_3 + \frac{674281}{4374} & \frac{9284531}{11664} - \frac{26}{27}f^2 - \frac{2798}{81}f - \left(20f + \frac{1921}{9}\right)\zeta_3 \\ -\frac{52}{81}f^2 - \frac{31175}{8748}f - \left(\frac{136f}{9} + \frac{3154}{81}\right)\zeta_3 + \frac{2951809}{52488} & \frac{3227801}{8748} - \frac{65}{54}f^2 - \frac{105293}{11664}f + \left(\frac{200}{27} - \frac{220}{9}f\right)\zeta_3 \\ \frac{272}{81}f^2 - \frac{27428}{81}f - \frac{13984}{27}\zeta_3 + \frac{14732222}{2187} & \frac{16521659}{2916} - \frac{316}{27}f^2 + \frac{8081}{54}f - \left(200f + \frac{22420}{9}\right)\zeta_3 \\ -\frac{1720}{243}f^2 + \frac{395783}{4374}f + \left(-\frac{1360}{9}f - \frac{33832}{81}\right)\zeta_3 - \frac{22191107}{13122} & -\frac{533}{81}f^2 + \frac{3353393}{5832}f + \left(\frac{9248}{27} - \frac{1120}{9}f\right)\zeta_3 - \frac{32043361}{8748} \end{pmatrix}. \tag{3.15}$$

Here and in the following, f is the number of active quark flavors.

We denote the anomalous dimension for the double insertion of either Q_+ or Q_- and one of the operators $Q_+, Q_-, Q_3, \ldots, Q_6$ by

$$\tilde{\gamma}^{T}_{\pm,7} = (\tilde{\gamma}_{\pm+,7}, \tilde{\gamma}_{\pm-,7}, \tilde{\gamma}_{\pm3,7}, \tilde{\gamma}_{\pm4,7}, \tilde{\gamma}_{\pm5,7}, \tilde{\gamma}_{\pm6,7}), \tag{3.16}$$

and find

$$\tilde{\gamma}^{T(0)}_{+,7} = (-3, 1, 0, 0, -96, -8), \qquad \tilde{\gamma}^{T(0)}_{-,7} = (1, -1, 0, 0, 48, -8), \tag{3.17}$$

$$\tilde{\gamma}^{T(1)}_{+,7} = \left(-30, 23, -\frac{140}{3}, -\frac{341}{9}, -\frac{248}{3}, \frac{1252}{9}\right), \qquad \tilde{\gamma}^{T(1)}_{-,7} = \left(23, -46, \frac{4}{3}, -\frac{101}{9}, -\frac{680}{3}, -\frac{164}{9}\right), \tag{3.18}$$

$$\begin{aligned}
\tilde{\gamma}^{T(2)}_{+,7} &= \left(\frac{5437543}{2808} - \frac{158279}{1950}f + 252\zeta_3, \frac{166441}{5850}f + \frac{106\zeta_3}{3} - \frac{8107577}{7020}, \frac{40}{9}f - \frac{472}{3}\zeta_3 + \frac{27909247}{7020},\right. \\
&\quad \left. \frac{578}{27}f - \frac{2698}{9}\zeta_3 + \frac{5333399}{3240}, \frac{225176}{195}f + \frac{6128}{3}\zeta_3 - \frac{9973214}{1755}, \frac{4712717}{1755}f + \frac{4856}{9}\zeta_3 - \frac{832816243}{10530}\right), \\
\tilde{\gamma}^{T(2)}_{-,7} &= \left(\frac{166441}{5850}f + \frac{106}{3}\zeta_3 - \frac{8107577}{7020}, \frac{93707}{5850}f + \frac{104}{3}\zeta_3 - \frac{23496713}{70200}, -\frac{32}{9}f + \frac{200}{3}\zeta_3 - \frac{30781813}{35100},\right. \\
&\quad \left. -\frac{94}{27}f - \frac{922}{9}\zeta_3 - \frac{31831601}{210600}, \frac{364552}{975}f + \frac{1328}{3}\zeta_3 - \frac{83770148}{1755}, \frac{1412938999}{52650} - \frac{6223223}{8775}f + \frac{4328}{9}\zeta_3\right),
\end{aligned} \tag{3.19}$$

at LO, NLO, and NNLO, respectively. The LO and NLO results agree with the literature [7] after the corresponding change of the operator basis, described in the Appendix. The NNLO result is new.

In the calculation of $\tilde{\gamma}_{S2}$ (cf. the diagrams in Fig.6) we have chosen the evanescent operators in the dimension-eight sector in such a way that the anomalous dimension of the operator $\tilde{Q}_{S2}$ equals the anomalous dimension of Q_+ through NNLO. Consequently $\tilde{\gamma}_{S2} = \gamma_+$, and [13]

$$\begin{aligned}
\gamma^{(0)}_+ &= 4, \\
\gamma^{(1)}_+ &= \frac{4}{9}f - 7, \\
\gamma^{(2)}_+ &= \frac{275267}{150} - \frac{52891}{675}f - \frac{260}{81}f^2 \\
&\quad - \left(\frac{160}{3}f + 672\right)\zeta_3.
\end{aligned} \tag{3.20}$$

The explicit expressions for the QCD β function and the anomalous dimension of the quark mass are given by [18–21]

$$\begin{aligned}
\beta_0 &= 11 - \frac{2}{3}f, \\
\beta_1 &= 102 - \frac{38}{3}f, \\
\beta_2 &= \frac{2857}{2} - \frac{5033}{18}f + \frac{325}{54}f^2,
\end{aligned} \tag{3.21}$$

and

$$\begin{aligned}
\gamma^{(0)}_m &= 8, \\
\gamma^{(1)}_m &= \frac{404}{3} - \frac{40}{9}f, \\
\gamma^{(2)}_m &= 2498 - \left(\frac{4432}{27} + \frac{320}{3}\zeta_3\right)f - \frac{280}{81}f^2.
\end{aligned} \tag{3.22}$$

C. Threshold corrections at the bottom-quark scale

When we pass the bottom-quark threshold, we must perform a proper matching between the effective theories with five and four flavors. This threshold correction is computed by requiring the equality of the Green's functions in the two theories at the matching scale, in

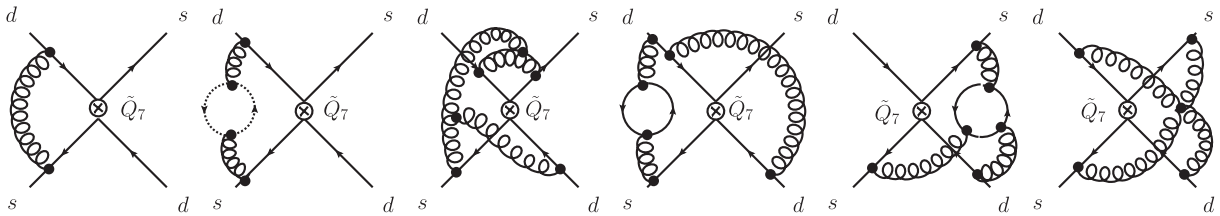

FIG. 6. Sample one-, two-, and three-loop diagrams, whose divergent parts contribute to the anomalous dimensions of the operator $\tilde{Q}_7$. Curly lines denote gluons, dotted lines denote ghosts, and solid lines denote quarks.

this case $\mu_b = \mathcal{O}(m_b)$, where m_b is the bottom-quark mass.

At NNLO, there are several sources of matching corrections. The penguin operators are affected already at NLO, because they explicitly depend on the number of light-quark fields. At NNLO also the matching of the current-current and the dimension-eight operators is nontrivial. The source of such contributions are virtual bottom quarks in two-loop matrix elements of the form shown in Fig. 7. In addition, also the strong coupling constant and the charm-quark mass are discontinuous beyond LO.

Let us write the equality of a general amplitude in the two theories at the matching scale μ_f as

$$C_{f-1}(\mu_f)\langle Q_{f-1}\rangle(\mu_f) = C_f(\mu_f)\langle Q_f\rangle(\mu_f), \tag{3.23}$$

the variables with subscripts f and $f-1$ belonging to the f- and $f-1$-flavor theory. At the bottom-quark scale, we have $f = 5$. We parametrize the matrix elements of the operators as an expansion in the coupling constant defined in the corresponding f-flavor theory:

$$\langle Q_f\rangle(\mu_f) = \left(1 + \frac{\alpha_s^{(f)}(\mu_f)}{4\pi} r_f^{(1)}(\mu_f) + \left(\frac{\alpha_s^{(f)}(\mu_f)}{4\pi}\right)^2 r_f^{(2)}(\mu_f)\right)\langle Q_f\rangle^{(0)}. \tag{3.24}$$

An additional subtlety arises, because the strong coupling constant also gets a nontrivial matching correction at a flavor threshold. Up to the NNLO approximation we have the relation [22–24]

$$\alpha_s^{(f)}(\mu_f) = \alpha_s^{(f-1)}(\mu_f)\left(1 + \frac{\alpha_s^{(f-1)}(\mu_f)}{4\pi}\frac{2}{3}\log\frac{\mu_f^2}{m_f^2} - \left(\frac{\alpha_s^{(f-1)}(\mu_f)}{4\pi}\right)^2\left(\frac{22}{9} - \frac{22}{3}\log\frac{\mu_f^2}{m_f^2} - \frac{4}{9}\log^2\frac{\mu_f^2}{m_f^2}\right)\right), \tag{3.25}$$

which we use to express all quantities in terms of the coupling constant $\alpha_s^{(f-1)}(\mu_f)$ in the effective theory with $f-1$ flavors. Here $m_f = m_f(\mu_f)$ is the $\overline{\text{MS}}$ mass of the quark which is integrated out. Note that the matching for $\tilde{C}_7$ starts at order $1/\alpha_s$, so that by inverting Eq. (3.25) we get a contribution already at NLO. Similarly, we need the decoupling relation for the charm-quark mass up to NNLO [25]:

$$m_c^{(f-1)}(\mu_f) = m_c^{(f)}(\mu_f)\left[1 + \left(\frac{\alpha_s^{(f)}(\mu_f)}{4\pi}\right)^2 \times \left(\frac{89}{27} - \frac{20}{9}\log\frac{\mu_f^2}{m_f^2} + \frac{4}{3}\log^2\frac{\mu_f^2}{m_f^2}\right)\right]. \tag{3.26}$$

In order to display the threshold corrections explicitly, we now introduce the discontinuities

$$\begin{aligned}\delta C^{(k)}(\mu_f) &= C_f^{(k)}(\mu_f) - C_{f-1}^{(k)}(\mu_f),\\ \delta r^{(k)}(\mu_f) &= r_f^{(k)}(\mu_f) - r_{f-1}^{(k)}(\mu_f),\end{aligned} \tag{3.27}$$

of the Wilson coefficients and the matrix elements, respectively, and find for the general solution of Eq. (3.23), in case of the dimension-six Wilson coefficients,

$$\begin{aligned}\delta C^{(0)}(\mu_f) &= 0,\\ \delta C^{(1)}(\mu_f) &= -C_f^{(0)}(\mu_f)\delta r^{(1)}(\mu_f),\\ \delta C^{(2)}(\mu_f) &= -C_f^{(1)}(\mu_f)\left(\delta r^{(1)}(\mu_f) + \frac{2}{3}\log\frac{\mu_f^2}{m_f^2}\right)\\ &\quad - C_f^{(0)}(\mu_f)\left(\delta r^{(2)}(\mu_f) - \delta r^{(1)}(\mu_f) r_{f-1}^{(1)}(\mu_f) + \frac{2}{3} r_f^{(1)}(\mu_f)\log\frac{\mu_f^2}{m_f^2}\right).\end{aligned} \tag{3.28}$$

Notice that the different single contributions in the last bracket may not be finite because of spurious IR divergences, which nevertheless cancel in the sum. The matching corrections look different for the dimension-eight Wilson coefficients, because of the factor $1/g^2$ in front of the operator:

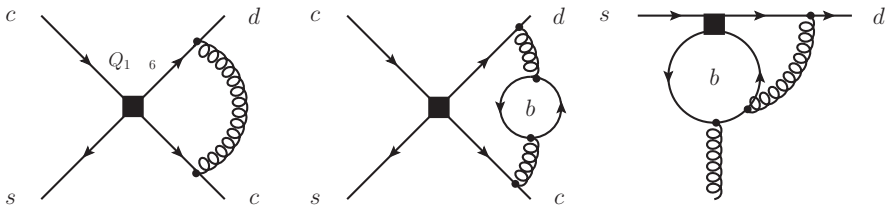

FIG. 7. Feynman diagrams relevant for the threshold corrections at the bottom-quark scale. The one-loop diagram of Q_1 and Q_2 is the same in both theories, whereas at the two-loop level they receive nontrivial corrections from virtual bottom quarks. The same applies to insertions of the operator $\tilde{Q}_7$. Because the penguin operators mix into Q_{EOM}, we also had to calculate insertions of $Q_{3,\ldots,6}$ with one external gluon, expanding up to the second power in the external momenta.

$$\delta\tilde{C}^{(0)}(\mu_f) = 0,$$
$$\delta\tilde{C}^{(1)}(\mu_f) = -\tilde{C}_f^{(0)}(\mu_f)\left(\delta\tilde{r}^{(1)}(\mu_f) - \frac{2}{3}\log\frac{\mu_f^2}{m_f^2}\right),$$
$$\delta\tilde{C}^{(2)}(\mu_f) = -\tilde{C}_f^{(1)}(\mu_f)\delta\tilde{r}^{(1)}(\mu_f) - \tilde{C}_f^{(0)}(\mu_f) \times\left[\delta\tilde{r}^{(2)}(\mu_f) - \left(\delta\tilde{r}^{(1)}(\mu_f) - \frac{2}{3}\log\frac{\mu_f^2}{m_f^2}\right) \times\tilde{r}_{f-1}^{(1)}(\mu_f) + \frac{22}{9} - \frac{22}{3}\log\frac{\mu_f^2}{m_f^2}\right]. \quad (3.29)$$

In addition, we have to take into account the terms related to the decoupling of the charm-quark mass.

At NLO, only the matrix elements of the penguin operators get nonvanishing contributions. They can be obtained from

$$\delta r_Q^{(1)}(\mu_b) = \begin{pmatrix} 0&0&0&0&0&0\\ 0&0&0&0&0&0\\ 0&0&0&0&0&0\\ 0&0&0&-\frac{2}{3}\log\frac{\mu_b^2}{m_b^2}&0&0\\ 0&0&0&0&0&0\\ 0&0&0&4-\frac{20}{3}\log\frac{\mu_b^2}{m_b^2}&0&0 \end{pmatrix}, \quad (3.30)$$

where δr_Q denotes the difference of the matrix elements in the subspace of dimension-six operators. At NNLO, we obtain the following contributions for the penguin operators:

$$\delta r_Q^{(2)}(\mu_b) - \delta r_Q^{(1)}(\mu_b) r_{Q,f=4}^{(1)}(\mu_b) + \frac{2}{3} r_{Q,f=5}^{(1)}(\mu_b)\log\frac{\mu_b^2}{m_b^2} = \begin{pmatrix} a_+^{(2)}&0&0&0&0&0\\ 0&a_-^{(2)}&0&0&0&0\\ 0&0&a_{33}^{(2)}&a_{34}^{(2)}&a_{35}^{(2)}&a_{36}^{(2)}\\ 0&0&a_{43}^{(2)}&a_{44}^{(2)}&a_{45}^{(2)}&a_{46}^{(2)}\\ 0&0&a_{53}^{(2)}&a_{54}^{(2)}&a_{55}^{(2)}&a_{56}^{(2)}\\ 0&0&a_{63}^{(2)}&a_{64}^{(2)}&a_{65}^{(2)}&a_{66}^{(2)} \end{pmatrix}, \quad (3.31)$$

where we can extract $a_+^{(2)}$ and $a_-^{(2)}$ from [13] to find

$$a_\pm^{(2)} = \delta r_\pm^{(2)}(\mu_b) = \mp\left(1 \mp \frac{1}{3}\right)\left(\frac{59}{36} + \frac{1}{3}L_b + L_b^2\right) \quad (3.32)$$

($L_b = \log(\mu_b^2/m_b^2)$ here and in the following two equations). We have determined the other entries by calculating two-loop matrix elements of the operators Q_+, Q_-, $Q_{3\ldots6}$ between appropriate external states [see Fig. 7], and find

$$\begin{aligned} a_{33}^{(2)} &= 0,\\ a_{34}^{(2)} &= \frac{443}{54} - \frac{10}{9}L_b + \frac{10}{3}L_b^2,\\ a_{35}^{(2)} &= 0,\\ a_{36}^{(2)} &= -\frac{85}{108} + \frac{1}{9}L_b - \frac{1}{3}L_b^2;\\ a_{43}^{(2)} &= \frac{886}{243} - \frac{184}{81}L_b + \frac{40}{27}L_b^2,\\ a_{44}^{(2)} &= \frac{589}{162} - \frac{370}{81}L_b + \frac{37}{54}L_b^2,\\ a_{45}^{(2)} &= -\frac{85}{243} + \frac{4}{81}L_b - \frac{4}{27}L_b^2,\\ a_{46}^{(2)} &= -\frac{425}{648} + \frac{5}{54}L_b - \frac{5}{18}L_b^2;\\ a_{53}^{(2)} &= -\frac{452}{27} + \frac{80}{9}L_b,\\ a_{54}^{(2)} &= \frac{565}{27} + \frac{740}{9}L_b + \frac{100}{3}L_b^2,\\ a_{55}^{(2)} &= \frac{38}{27} - \frac{8}{9}L_b,\\ a_{56}^{(2)} &= -\frac{383}{54} - \frac{74}{9}L_b - \frac{10}{3}L_b^2;\\ a_{63}^{(2)} &= \frac{6874}{243} - \frac{88}{81}L_b + \frac{328}{27}L_b^2,\\ a_{64}^{(2)} &= -\frac{2651}{162} + \frac{5030}{81}L_b - \frac{220}{27}L_b^2,\\ a_{65}^{(2)} &= -\frac{826}{243} - \frac{128}{81}L_b - \frac{40}{27}L_b^2,\\ a_{66}^{(2)} &= -\frac{467}{162} - \frac{266}{27}L_b - \frac{23}{18}L_b^2. \end{aligned} \quad (3.33)$$

For the dimension-eight operator we find the only nonvanishing contribution

$$\delta\tilde{r}_7^{(2)}(\mu_b) = -\frac{59}{54} - \frac{2}{9}L_b - \frac{2}{3}L_b^2 = \delta r_+^{(2)}(\mu_b). \quad (3.34)$$

D. Matching at the charm-quark scale

At the scale $\mu_c = \mathcal{O}(m_c)$ the charm quark is removed from the theory as a dynamical degree of freedom, and the effective Lagrangian is now given by Eq. (2.15). Requiring the equality of the Green's functions in both theories at the charm-quark scale leads to the matching condition

$$\sum_{i,k=+,-}\sum_{j,l=+,-,3}^{6} C_i(\mu_c)C_j(\mu_c)Z_{ik}Z_{jl}\langle Q_k Q_l\rangle(\mu_c) + \tilde{C}_7(\mu_c)\tilde{Z}_{77}\langle\tilde{Q}_7\rangle(\mu_c) = \frac{1}{32\pi^2}\tilde{C}_{S2}^{ct}(\mu_c)\tilde{Z}_{S2}\langle\tilde{Q}_{S2}\rangle(\mu_c), \quad (3.35)$$

which we use to determine the Wilson coefficient $\tilde{C}_{S2}^{ct}(\mu)$. To proceed, we parametrize the matrix elements in the following way:

$$\begin{aligned}\langle\tilde{Q}_7\rangle &= r_7\langle\tilde{Q}_7\rangle^{(0)},\\ \langle\tilde{Q}_{S2}\rangle &= r_{S2}\langle\tilde{Q}_{S2}\rangle^{(0)}, \quad \text{and}\\ \langle Q_iQ_j\rangle(\mu_c) &= \frac{m_c^2(\mu_c)}{32\pi^2} r_{ij,S2}\langle\tilde{Q}_{S2}\rangle^{(0)}.\end{aligned} \tag{3.36}$$

If we take into account the explicit factor of m_c^2/g^2 in the definition of $\tilde{Q}_7$ and expand the Wilson coefficient $\tilde{C}_{S2}^{ct}$ as

$$\begin{aligned}\tilde{C}_{S2}^{ct}(\mu) = &\frac{4\pi}{\alpha_s^{(3)}(\mu)}\tilde{C}_{S2}^{ct(0)}(\mu) + \tilde{C}_{S2}^{ct(1)}(\mu)\\ &+ \frac{\alpha_s^{(3)}(\mu)}{4\pi}\tilde{C}_{S2}^{ct(2)}(\mu),\end{aligned} \tag{3.37}$$

we find the following contributions to the matching:

$$\tilde{C}_{S2}^{ct(0)}(\mu_c) = 2m_c^2(\mu_c)\tilde{C}_7^{(0)}(\mu_c), \tag{3.38}$$

$$\begin{aligned}\tilde{C}_{S2}^{ct(1)}(\mu_c) = &2m_c^2(\mu_c)\Big[\tilde{C}_7^{(0)}(\mu_c)\Big(r_7^{(1)} - r_{S2}^{(1)}\\ &- \frac{2}{3}\log\frac{\mu_c^2}{m_c(\mu_c)^2}\Big) + \tilde{C}_7^{(1)}(\mu_c)\Big]\\ &+ m_c^2(\mu_c)C_i^{(0)}(\mu_c)C_j^{(0)}(\mu_c)r_{ij,S2}^{(0)},\end{aligned} \tag{3.39}$$

$$\begin{aligned}\tilde{C}_{S2}^{ct(2)}(\mu_c) = &2m_c^2(\mu_c)\Big[\tilde{C}_7^{(0)}(\mu_c)\Big(\delta\tilde{r}_7^{(2)}(\mu_c) + \frac{22}{9}\\ &- \frac{22}{3}\log\frac{\mu_c^2}{m_c(\mu_c)^2}\Big) + \tilde{C}_7^{(2)}(\mu_c)\Big]\\ &+ m_c^2(\mu_c)\Big[C_i^{(0)}(\mu_c)C_j^{(0)}(\mu_c)\Big(r_{ij,S2}^{(1)} - r_{ij,S2}^{(0)}r_{S2}^{(1)}\Big)\\ &+ C_i^{(0)}(\mu_c)C_j^{(1)}(\mu_c)r_{ij,S2}^{(0)}\\ &+ C_i^{(1)}(\mu_c)C_j^{(0)}(\mu_c)r_{ij,S2}^{(0)}\Big],\end{aligned} \tag{3.40}$$

where $\delta\tilde{r}_7^{(2)}(\mu_c)$ is given by Eq. (3.34), with μ_b and m_b replaced by μ_c and m_c, respectively. Notice the additional logarithms which we get by expressing $\alpha_s^{(f=4)}$ through $\alpha_s^{(f=3)}$. These terms, which are numerically tiny at NLO, have been neglected in Ref. [7].

Furthermore, we expand the charm-quark mass defined at the scale μ_c, viz. $m_c(\mu_c)$, about $m_c(m_c)$ (see [13]):

$$x_c(\mu_c) = \kappa_c\Big(1 + \frac{\alpha_s^{(4)}(\mu_c)}{4\pi}\xi_c^{(1)} + \Big(\frac{\alpha_s^{(4)}(\mu_c)}{4\pi}\Big)^2\xi_c^{(2)}\Big)x_c(m_c). \tag{3.41}$$

Here $\kappa_c = \eta_c^{24/25}$ with $\eta_c = \alpha_s^{(4)}(\mu_c)/\alpha_s^{(4)}(m_c)$ and

$$\begin{aligned}\xi_c^{(1)} &= \frac{15212}{1875}(1 - \eta_c^{-1}),\\ \xi_c^{(2)} &= \frac{966966391}{10546875} - \frac{231404944}{3515625}\eta_c^{-1}\\ &\quad - \frac{272751559}{10546875}\eta_c^{-2} - \frac{128}{5}(1 - \eta_c^{-2})\zeta_3.\end{aligned} \tag{3.42}$$

In order to evaluate the Eqs. (3.38), (3.39), and (3.40), we have to compute the finite parts of one- and two-loop Feynman diagrams of the type shown in Fig. 8. In this way we find for $r_{\pm j,S2}$ at one loop

$$r_{\pm j,S2}^{(0),T}(\mu_c) = \begin{pmatrix} 3\log\left(\frac{\mu_c^2}{m_c^2}\right) - \frac{3}{2} & \frac{1}{2} - \log\left(\frac{\mu_c^2}{m_c^2}\right)\\ \frac{1}{2} - \log\left(\frac{\mu_c^2}{m_c^2}\right) & \log\left(\frac{\mu_c^2}{m_c^2}\right) - \frac{1}{2}\\ 0 & 0\\ 0 & 0\\ 96\log\left(\frac{\mu_c^2}{m_c^2}\right) + 224 & -48\log\left(\frac{\mu_c^2}{m_c^2}\right) - 112\\ 8\log\left(\frac{\mu_c^2}{m_c^2}\right) + \frac{56}{3} & 8\log\left(\frac{\mu_c^2}{m_c^2}\right) + \frac{56}{3}\end{pmatrix}. \tag{3.43}$$

This result agrees with the one obtained in [7] after the appropriate basis transformation. A two-loop matching calculation yields

$$(r_{\pm j,S2}^{(1),T} - r_{\pm j,S2}^{(0),T}r_{S2}^{(1)})(\mu_c) = \begin{pmatrix} 9\log^2\left(\frac{\mu_c^2}{m_c^2}\right) - 3\log\left(\frac{\mu_c^2}{m_c^2}\right) - \zeta_2 + \frac{54926}{325} & -6\log^2\left(\frac{\mu_c^2}{m_c^2}\right) - 9\log\left(\frac{\mu_c^2}{m_c^2}\right) + \frac{5}{3}\zeta_2 - \frac{89497}{1300}\\ -6\log^2\left(\frac{\mu_c^2}{m_c^2}\right) - 9\log\left(\frac{\mu_c^2}{m_c^2}\right) + \frac{5}{3}\zeta_2 - \frac{89497}{1300} & 9\log^2\left(\frac{\mu_c^2}{m_c^2}\right) + 29\log\left(\frac{\mu_c^2}{m_c^2}\right) + \frac{1}{3}\zeta_2 + \frac{11664}{325}\\ -4\log^2\left(\frac{\mu_c^2}{m_c^2}\right) + 28\log\left(\frac{\mu_c^2}{m_c^2}\right) + \frac{23}{3} & -4\log^2\left(\frac{\mu_c^2}{m_c^2}\right) - 20\log\left(\frac{\mu_c^2}{m_c^2}\right) - \frac{37}{3}\\ -\frac{37}{3}\log^2\left(\frac{\mu_c^2}{m_c^2}\right) - \frac{59}{3}\log\left(\frac{\mu_c^2}{m_c^2}\right) - \frac{1531}{36} & \frac{11}{3}\log^2\left(\frac{\mu_c^2}{m_c^2}\right) + \frac{85}{3}\log\left(\frac{\mu_c^2}{m_c^2}\right) + \frac{917}{36}\\ 344\log^2\left(\frac{\mu_c^2}{m_c^2}\right) + 920\log\left(\frac{\mu_c^2}{m_c^2}\right) - \frac{64878}{65} & -376\log^2\left(\frac{\mu_c^2}{m_c^2}\right) - 1144\log\left(\frac{\mu_c^2}{m_c^2}\right) - \frac{964226}{325}\\ -\frac{220}{3}\log^2\left(\frac{\mu_c^2}{m_c^2}\right) - \frac{1636}{3}\log\left(\frac{\mu_c^2}{m_c^2}\right) - \frac{1015087}{195} & \frac{332}{3}\log^2\left(\frac{\mu_c^2}{m_c^2}\right) + \frac{1412}{3}\log\left(\frac{\mu_c^2}{m_c^2}\right) + \frac{503161}{325}\end{pmatrix}. \tag{3.44}$$

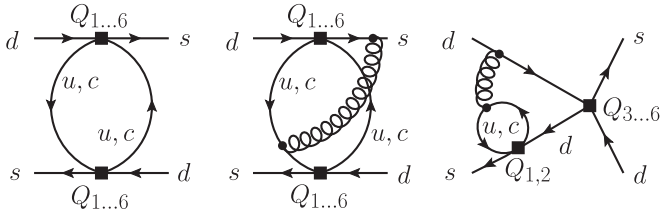

FIG. 8. Sample one- and two-loop diagrams contributing to the matching at the charm-quark scale.

This result is new and completes the matching onto the three-flavor theory. Now only a single operator contributes, and the renormalization group evolution below the charm-quark scale is the same for the top-, the charm-, and the charm-top-quark contribution.

E. Renormalization group equations below the charm-quark threshold

The effective Hamiltonian valid below the charm-quark threshold contains only the single operator $\tilde{Q}_{S2}$. The renormalization group evolution is now the same for the three Wilson coefficients $\tilde{C}^j_{S2}$, where $j = c, t, ct$, and is described by the evolution matrix corresponding to the anomalous dimension of $\tilde{Q}_{S2}$:

$$\tilde{C}^{\,j}_{S2}(\mu) = U(\mu, \mu_c)\tilde{C}^j_{S2}(\mu_c). \tag{3.45}$$

By comparing (1.5) and (2.15), we see that we can express the coefficients η_{cc}, η_{tt}, η_{ct} as

$$\eta_{cc} = \frac{1}{m_c^2(m_c)}\tilde{C}^{(c)}_{S2}(\mu_c)[\alpha_s^{(3)}(\mu_c)]^{a_+}K_+^{-1}(\mu_c), \tag{3.46a}$$

$$\eta_{tt} = \frac{1}{M_W^2 S(x_t(m_t))}\tilde{C}^{(t)}_{S2}(\mu_c)[\alpha_s^{(3)}(\mu_c)]^{a_+}K_+^{-1}(\mu_c), \tag{3.46b}$$

$$\eta_{ct} = \frac{1}{2M_W^2 S(x_c(m_c), x_t(m_t))}\tilde{C}^{(ct)}_{S2}(\mu_c)[\alpha_s^{(3)}(\mu_c)]^{a_+}K_+^{-1}(\mu_c). \tag{3.46c}$$

The remaining μ dependence present in (3.46), corresponding to the lower end of the evolution in Eq. (3.45), is absorbed into $b(\mu)$, which equals

$$b(\mu) = [\alpha_s^{(3)}(\mu)]^{-a_+}K_+(\mu), \tag{3.47}$$

where

$$K_+(\mu) = \left(1 + J_+^{(1)}\frac{\alpha_s^{(3)}(\mu)}{4\pi} + J_+^{(2)}\left(\frac{\alpha_s^{(3)}(\mu)}{4\pi}\right)^2\right), \tag{3.48}$$

and the exponent a_+ is the so-called *magic number* for the operator Q_+ (the magic numbers as well as the matrix J are defined for instance in [4]). This scale dependence is cancelled by the corresponding scale dependence of the hadronic matrix element.

F. Analytical checks of our calculation

Because the calculation of the NNLO contributions to η_{ct} is quite complex, we checked our results in several ways.

First of all the calculation of the $\mathcal{O}(100000)$ Feynman diagrams as well as the renormalization, the computation of the anomalous dimensions, and the matching, has been performed independently by the two of us, using a completely different setup of computer programs. On the one hand we use QGRAF [26] for generating the diagrams; the evaluation of the integrals is then performed using the program packages Q2E/EXP/MATAD [27,28], where MATAD is written in FORM [29] and based on the integration-by-parts algorithm [30,31]. In addition, we have written our own FORM routine in order to evaluate two-loop diagrams with an arbitrary number of (possibly vanishing) masses, using the algorithm described in [14,32]. On the other hand, all calculations have been performed using a completely independent setup, based on FEYNARTS [33] and MATHEMATICA.

As a check of our calculation, we verified that all anomalous dimensions, Wilson coefficients, and matrix elements are independent of the gauge-fixing parameter ξ. Because of the complexity of the analytical expressions, for the three-loop penguin insertions we kept only the first power in ξ for our check.

Another very useful check is the locality of the counterterms, which is an implication of renormalizability. In a mass independent renormalization scheme this means that the renormalization factors Z depend on μ only through the coupling constants. We have checked this explicitly and found μ independence of all our renormalization constants.

We have also checked analytically that η_{ct} is independent of the matching scales μ_W, μ_b, and μ_c to the considered order of the strong coupling constant, by expanding the full solution of the renormalization group equations about the respective matching scale.

As a cross-check, we confirm the NLO results of Herrlich and Nierste [7] for the first time.

IV. DISCUSSION AND NUMERICS

In this section we present the numerical value of η_{ct} at NNLO and discuss the theoretical uncertainty, as well as the impact on ϵ_K. Our input parameters are collected in Table I.

The theoretical uncertainty of η_{ct} is related to the truncation of the perturbation series. We estimate it by consid-

TABLE I. Input parameters used in our numerical analysis.

Parameter	Value	Ref.	Parameter	Value	Ref.
M_W	80.399(23) GeV	[2]	$\alpha_s(M_Z)$	0.1184(7)	[2]
$m_t(m_t)$	163.7(1.1) GeV	[34]	F_K	156.1(8) MeV	[35]
$m_b(m_b)$	4.163(16) GeV	[36]	G_F	$1.166367(5) \times 10^{-5}$ GeV^{-2}	[2]
$m_c(m_c)$	1.286(13) GeV	[36]	λ	0.2255(7)	[35]
M_K	497.614(24) MeV	[2]	$\lvert V_{cb}\rvert$	$4.06(13) \times 10^{-2}$	[2]
κ_ϵ	0.94(2)	[3]	M_{B_d}	5.2795(3) GeV	[2]
ΔM_K	5.292(9)/ns	[2]	M_{B_s}	5.3663(6) GeV	[2]
ΔM_d	0.507(5)/ps	[2]	ΔM_s	17.77(12)/ps	[2]
ξ_s	1.243(28)	[9]	η_{tt}	0.5765(65)	[8]
$\hat{B}_K$	0.725(26)	[9]	η_{cc}	1.43(23)	[7]
$\sin 2\beta$	0.671(23)	[2]			

ering the remaining scale dependence, the different methods to evaluate the running strong coupling constant, and the size of the NNLO corrections. Varying μ_c from 1 to 2 GeV and μ_W from 40 to 200 GeV, we find the following numerical value at NNLO:

$$\eta_{ct} = 0.496 \pm 0.045_{\mu_c} \pm 0.013_{\mu_W} \pm 0.002_{\alpha_s} \pm 0.001_{m_c} \pm 0.0002_{m_t}, \tag{4.1}$$

where we also display the parametric uncertainties stemming from the experimental error on α_s, m_c, and m_t. The dependence on the scale μ_b is completely negligible.

The dependence on the electroweak matching scale μ_W is shown in Fig. 9. We have plotted η_{ct} as a function of μ_W in the range from 40 GeV to 200 GeV, where we fixed the other scales as $\mu_b = 5$ GeV and $\mu_c = 1.5$ GeV, respectively. The relatively weak residual dependence on μ_W at NLO is slightly increased at NNLO. By contrast, the dependence on μ_b, which is shown in Fig. 10, fixing $\mu_W = 80$ GeV and $\mu_c = 1.5$ GeV, is completely negligible. The dependence on the scale μ_c is shown in Fig. 11, where we vary μ_c in the range from 1 to 2 GeV, fixing $\mu_W = 80$ GeV and $\mu_b = 5$ GeV. In addition, we have plotted η_{ct} corresponding to three different possibilities of calculating

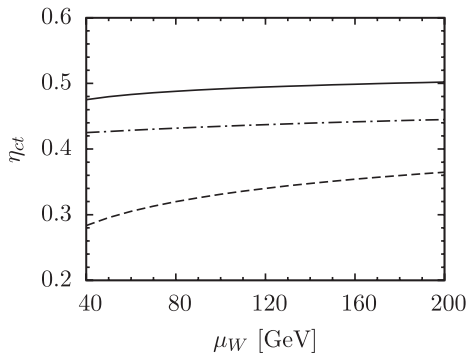

FIG. 9. η_{ct} as a function of μ_W at LO (dashed line), NLO (dash-dotted line), and NNLO QCD (solid line).

$\alpha_s(\mu_c)$ from the experimental input value of $\alpha_s(M_Z)$: One method (method 1) is to solve the renormalization group equation for α_s numerically. Furthermore, it is possible to compute α_s by first determining the scale parameter $\Lambda_{\rm QCD}$. This can be achieved by using the explicit solution for $\Lambda_{\rm QCD}$ without expansion in α_s (method 2) or by iteratively solving this equation for $\Lambda_{\rm QCD}$ and from this value determining α_s (method 3). The dashed, dotted, and dash-dotted lines in Fig. 11, each of them representing the NLO result for η_{ct}, correspond to these three possibilities of determining α_s, respectively. We used the MATHEMATICA package RUNDEC [37] for the numerical evaluation. Note that the difference between these three methods vanishes almost entirely at NNLO. On the other hand, at NLO the effect is sizeable and thus contributes to the theoretical uncertainty. Varying μ_c and μ_W in the same range as above, we find at NLO

$$\eta_{ct}^{\rm NLO} = 0.457 \pm 0.072_{\mu_c} \pm 0.01_{\mu_W} \pm 0.0001_{\alpha_s} \pm 0.002_{m_c} \pm 0.0003_{m_t}, \tag{4.2}$$

where there error indicated by the subscript μ_c includes the effect of the three ways of determining α_s. For the variation of the scale μ_W we have used only method 1 for evaluating α_s in order to avoid double-counting of the related uncertainty.[5] Again we have included the parametric uncertainties related to α_s, m_c, and m_t.

The authors of Ref. [7] have varied μ_c in the smaller range from 1.1 to 1.6 GeV, using a procedure equivalent to method 3 above for determining α_s. By looking at the explicit values of η_{ct} in Fig. 11 we see that the two error bands at NLO and NNLO, resulting from this smaller range of μ_c, have almost no overlap. Now, with the NNLO results at hand, we see that our range for μ_c leads to a better estimate of the theoretical uncertainty.

Looking at Fig. 11, it is striking that the scale dependence of the NLO result is barely reduced at NNLO. In order to understand this behavior, let us look at the remain-

[5]Otherwise the error would amount to $\pm 0.018_{\mu_W}$.

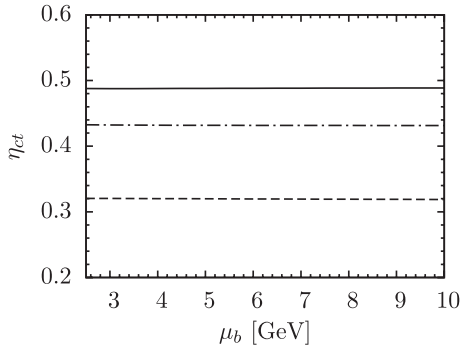

FIG. 10. η_{ct} as a function of μ_b at LO (dashed line), NLO (dash-dotted line), and NNLO QCD (solid line).

ing μ_c dependence, which is the most pronounced, in more detail. It originates from terms proportional to higher powers of α_s times logarithms of the renormalization scale that are contained in the explicit solutions of the renormalization group equations. These terms are only partially canceled due to our truncating the perturbative expansion of the matrix elements at the charm-quark scale.

We have separated the contributions to η_{ct} of the different Wilson coefficients multiplying the matrix elements at the charm-quark scale [cf. Eq. (3.38)]. To this end we have chosen the operator basis as in Ref. [7], where we use the diagonal operator basis only in one dimension-six subspace, and $Q_1, \ldots, Q_6$ in the other. It turns out that only one contribution, proportional to the combination $C_- C_2$, shows a strong scale dependence. Although the size of the individual contributions certainly depends on the chosen renormalization scheme, the general pattern is independent of this convention. It is related to the vanishing of the entry in the LO anomalous dimension tensor corresponding to the two operators Q_- and Q_2. This incidence leads to a behavior of the scale dependence for this single combination which would be expected from a NLO calculation, and dominates the scale dependence of the NNLO result.

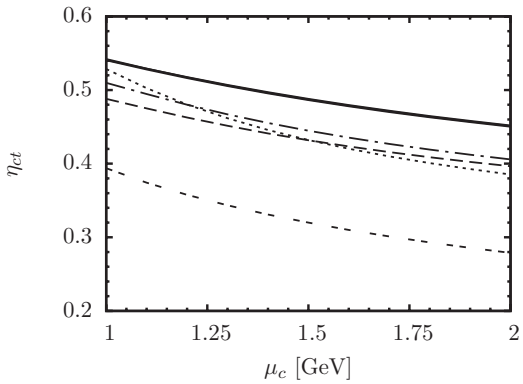

FIG. 11. η_{ct} as a function of μ_c. The LO result is represented by the double-dotted line. The dashed, dotted, and dash-dotted lines correspond to the NLO value of η_{ct}, with α_s evaluated by method 1, 2, and 3, explained in the text. The solid lines show the corresponding NNLO results; the ambiguity is almost canceled.

In general, the perturbation series for the $\Delta S = 2$ four-quark operator in an effective three-flavor theory is not expected to converge as well as, for instance, the perturbation series in Ref. [13], where the mixing into a semileptonic operator was calculated.

Finally we remark that the absolute value of the NNLO correction is of the same order of magnitude as the range of η_{ct} at NNLO in the interval $\mu_c = 1 \ldots 2$ GeV, so that using the size of the NNLO corrections as an estimate of the theoretical uncertainty yields approximately the same error as using the scale variation in the quoted interval.

As a summary of the discussion above, we give the following final estimate for the charm-top-quark contribution to ϵ_K at NNLO:

$$\eta_{ct} = 0.496 \pm 0.047. \tag{4.3}$$

(For comparison, an error estimate using a range for μ_c as in Ref. [7] would yield $\eta_{ct} = 0.504 \pm 0.025$.) The parametric uncertainty is essentially negligible with respect to the theoretical uncertainty. Compared to our NLO value,

$$\eta_{ct}^{\mathrm{NLO}} = 0.457 \pm 0.073, \tag{4.4}$$

this corresponds to a positive shift of approximately 7%.

Before we conclude this section, we study the impact of our calculation on the prediction of $|\epsilon_K|$. To this end we use the following formula[6] [38,39]:

$$|\epsilon_K| = \kappa_\epsilon C_\epsilon \hat{B}_K |V_{cb}|^2 \lambda^2 \bar{\eta} (|V_{cb}|^2 (1-\bar{\rho}) \eta_{tt} S(x_t) + \eta_{ct} S(x_c, x_t) - \eta_{cc} S(x_c)), \tag{4.5}$$

where

$$C_\epsilon = \frac{G_F^2 F_K^2 M_{K^0} M_W^2}{6\sqrt{2}\pi^2 \Delta M_K}. \tag{4.6}$$

We write $\bar{\eta} = R_t \sin\beta$ and $1 - \bar{\rho} = R_t \cos\beta$, where R_t is given by

$$R_t \approx \frac{\xi_s}{\lambda} \sqrt{\frac{M_{B_s}}{M_{B_d}}} \sqrt{\frac{\Delta M_d}{\Delta M_s}} \tag{4.7}$$

and $\xi_s = (F_{B_s}\sqrt{\hat{B}_s})/(F_{B_d}\sqrt{\hat{B}_d})$ is a ratio of B meson decay constants and bag factors that can be computed on the lattice with high precision [9]. Using the numerical values given in Table I, we obtain

$$|\epsilon_K| = (1.90 \pm 0.04_{\eta_{cc}} \pm 0.02_{\eta_{tt}} \pm 0.07_{\eta_{ct}} \pm 0.11_{\mathrm{LD}} \pm 0.22_{\mathrm{parametric}}) \times 10^{-3}. \tag{4.8}$$

The first three errors correspond to η_{cc}, η_{tt}, η_{ct}, respectively. The error indicated by LD originates from the

[6] A term proportional to $\mathrm{Re}\lambda_t/\mathrm{Re}\lambda_c = \mathcal{O}(\lambda^4)$ has been neglected in Eq. (4.5) (see Ref. [38]).

long-distance contribution, namely ξ_s, $\hat{B}_K$, and κ_ϵ, which account for 40%, 37%, and 22% of the long-distance error, respectively. The main share of the parametric error stems from $|V_{cb}|$ (59%) and $\sin(2\beta)$ (19%), while all other contributions are well below 10%. All errors have been added in quadrature.

Compared to the prediction using the NLO value η_{ct}^{NLO},

$$|\epsilon_K^{\mathrm{NLO}}| = (1.83 \pm 0.04_{\eta_{cc}} \pm 0.02_{\eta_{tt}} \pm 0.11_{\eta_{ct}} \pm 0.10_{\mathrm{LD}} \pm 0.22_{\mathrm{parametric}}) \times 10^{-3}, \tag{4.9}$$

this corresponds to a shift by approximately 3%.

V. CONCLUSION

We have performed a complete NNLO QCD analysis of the charm-top-quark contribution η_{ct} to the $|\Delta S| = 2$ effective Hamiltonian $\mathcal{H}_{f=3}^{|\Delta S|=2}$. We confirm the analytical results for η_{ct} obtained at NLO in Ref. [7] for the first time.

Some of our results are useful beyond η_{ct}. The anomalous dimension of the operator $\tilde{Q}_{S2}$ can be employed to compute the large NNLO logarithms of B^0-$\bar{B}^0$ mixing and comprise part of a NNLO calculation of η_{tt}. The NNLO matching corrections at the bottom-quark threshold have further applications in kaon physics.

Our numerical results for η_{ct} can be summarized by a 7% positive shift in the NNLO prediction with respect to the NLO value, leading to $\eta_{ct} = 0.496 \pm 0.047$. This corresponds to an enhancement of ϵ_K by roughly 3%, yielding $|\epsilon_K| = (1.90 \pm 0.26) \times 10^{-3}$. With our calculation we solidified the theory prediction of ϵ_K, strengthening its role as an important constraint for models of new physics.

ACKNOWLEDGMENTS

J. B. would like to thank Ulrich Nierste for suggesting the topic, Matthias Steinhauser for providing us with an updated version of MATAD, and Emmanuel Stamou for his help in improving our FORM routines. We also thank Ulrich Nierste for constant encouragement and discussions, and Andrzej Buras, Ulrich Nierste, Guido Bell, and Emmanuel Stamou for their careful reading of the manuscript. This research was supported by the DFG Cluster of Excellence "Origin and Structure of the Universe." The work of J. B. was supported by the EU Marie-Curie Grant No. MIRG-CT-2005-029152, BMBF Grant No. 05 HT6VKB, and by the DFG-funded Graduiertenkolleg Hochenergiephysik und Teilchenastrophysik at the University of Karlsruhe. M. G. thanks the Galileo Galilei Institute for Theoretical Physics for the hospitality and the INFN for partial support during the completion of this work.

APPENDIX: CHANGE OF THE OPERATOR BASIS

In this Appendix we examine how the Wilson coefficients and the anomalous dimensions transform under a change of the operator basis. This is important for two reasons: In order to find a compact form for the renormalization group equations for double operator insertions, we have seen it to be useful to work in a diagonal operator basis in the subspace of current-current operators. However, the calculation of the dimension-six anomalous dimensions and Wilson coefficients has been performed in the literature in the basis given in [4,12]. Moreover, we had to transform our results in order to compare them with results that are available in the literature and have been calculated using yet another operator basis [7].

As is well-known, a general change of the operator basis consists of a linear transformation and a corresponding change of the renormalization scheme [4]. Therefore, let us first as a preparation derive the transformation properties of the anomalous dimensions for an arbitrary change of the renormalization scheme. This generalizes the already known results. Suppose we perform the following change of scheme for the Wilson coefficients:

$$C_i \to C_i' = C_j \rho_{ji}^{-1}, \tag{A1}$$

$$\tilde{C}_k \to \tilde{C}_k' = \tilde{C}_j \tilde{\rho}_{jk}^{-1} - C_l C_m \hat{\rho}_{lm,k}. \tag{A2}$$

As before, we have denoted Wilson coefficients belonging to dimension-eight operators with a tilde and those belonging to dimension-six operators without superscript. Furthermore, we introduced the parameters ρ, $\tilde{\rho}$ and $\hat{\rho}$, which parametrize the finite transformations

$$\rho_{ij} = \delta_{ij} - \frac{\alpha_s}{4\pi}\rho_{ij}^{(1)} - \left(\frac{\alpha_s}{4\pi}\right)^2 (\rho_{ij}^{(2)} - \rho_{ik}^{(1)}\rho_{kj}^{(1)}) + \mathcal{O}(\alpha_s^3), \tag{A3}$$

$$\tilde{\rho}_{ij} = \delta_{ij} - \frac{\alpha_s}{4\pi}\tilde{\rho}_{ij}^{(1)} - \left(\frac{\alpha_s}{4\pi}\right)^2 (\tilde{\rho}_{ij}^{(2)} - \tilde{\rho}_{ik}^{(1)}\tilde{\rho}_{kj}^{(1)}) + \mathcal{O}(\alpha_s^3), \tag{A4}$$

$$\hat{\rho}_{lm,k} = \frac{\alpha_s}{4\pi}\hat{\rho}_{lm,k}^{(1)} + \left(\frac{\alpha_s}{4\pi}\right)^2 \hat{\rho}_{lm,k}^{(2)} + \mathcal{O}(\alpha_s^3). \tag{A5}$$

Then, in order for the effective Hamiltonian of the form

$$H_{\mathrm{eff}} = C_i Z_{ij} Q_j + (\tilde{C}_i \tilde{Z}_{ik} + C_i C_j \hat{Z}_{ij,k})\tilde{Q}_k \tag{A6}$$

to stay invariant, the renormalization constants must transform as

$$Z_{ij} \to Z_{ij}' = \rho_{ik} Z_{kj}, \tag{A7}$$

$$\tilde{Z}_{ij} \to \tilde{Z}_{ij}' = \tilde{\rho}_{ik} \tilde{Z}_{kj}, \tag{A8}$$

$$\hat{Z}_{ij,k} \to \hat{Z}_{ij,k}' = \rho_{il}\rho_{jm}\hat{Z}_{lm,k} + \rho_{il}\rho_{jm}\hat{\rho}_{lm,p}\tilde{\rho}_{pq}\tilde{Z}_{qk}. \tag{A9}$$

The transformation of the anomalous dimensions can now be obtained by inserting the transformed renormalization constants into the defining equation for the anomalous dimension matrix (3.5), and the anomalous dimension

tensor (3.7), respectively. In this way we obtain the well-known results for the case of single insertions [4,40,41]:

$$\gamma'^{(0)} = \gamma^{(0)}, \tag{A10}$$

$$\gamma'^{(1)} = \gamma^{(1)} - [\rho^{(1)}, \gamma^{(0)}] - 2\beta_0\rho^{(1)}, \tag{A11}$$

$$\gamma'^{(2)} = \gamma^{(2)} - [\rho^{(2)}, \gamma^{(0)}] - [\rho^{(1)}, \gamma^{(1)}] + \rho^{(1)}[\rho^{(1)}, \gamma^{(0)}] - 4\beta_0\rho^{(2)} - 2\beta_1\rho^{(1)} + 2\beta_0\rho^{(1)}\rho^{(1)}. \tag{A12}$$

The general transformation law for the anomalous dimension tensor for double insertion reads[7]

$$\hat{\gamma}'^{(0)}_{ij,k} = \gamma^{(0)}_{ij,k}, \tag{A13}$$

$$\hat{\gamma}'^{(1)}_{ij,k} = \gamma^{(1)}_{ij,k} + \hat{\rho}^{(1)}_{ij,l}\tilde{\gamma}^{(0)}_{lk} + 2\hat{\rho}^{(1)}_{ij,k}\beta_0 + \hat{\gamma}^{(0)}_{ij,l}\tilde{\rho}^{(1)}_{lk} - \left\{\gamma^{(0)}_{il}\delta_{jm} + \delta_{il}\gamma^{(0)}_{jm}\right\}\hat{\rho}^{(1)}_{lm,k} - \left\{\rho^{(1)}_{il}\delta_{jm} + \delta_{il}\rho^{(1)}_{jm}\right\}\hat{\gamma}^{(0)}_{lm,k}. \tag{A14}$$

Let us now examine how the anomalous dimensions and the Wilson coefficients change under a basis transformation. In four space-time dimensions, a change of n dimension-six operators Q and m dimension-eight operators $\tilde{Q}$ is simply given by a linear transformation

$$Q_i \to Q'_i = R_{ij}Q_j, \qquad \tilde{Q}_i \to \tilde{Q}'_i = \tilde{R}_{ij}\tilde{Q}_j, \tag{A15}$$

described by matrices $R \in \mathrm{GL}(n)$, $\tilde{R} \in \mathrm{GL}(m)$. Under this transformation the renormalization constants change according to

$$\begin{aligned} Z'_{ij} &= R_{ik}Z_{kl}R^{-1}_{lj}, \\ \tilde{Z}'_{ij} &= \tilde{R}_{ik}\tilde{Z}_{kl}\tilde{R}^{-1}_{lj}, \\ \hat{Z}'_{kn,l} &= R_{kk'}R_{nn'}\hat{Z}_{k'n',l'}\tilde{R}^{-1}_{l'l}. \end{aligned} \tag{A16}$$

In general, the situation is more complicated because of the presence of evanescent operators. As explained in detail in Ref. [4], a change of the operator basis consists of a linear transformation and a finite renormalization; the latter is needed in order to restore the standard $\overline{\mathrm{MS}}$ definition of the renormalization constants.

We can write a general transformation among all dimension-six operators as

$$\begin{pmatrix} Q' \\ E' \end{pmatrix} = \begin{pmatrix} R & 0 \\ 0 & M \end{pmatrix}\begin{pmatrix} 1 & 0 \\ \epsilon U + \epsilon^2 V & 1 \end{pmatrix}\begin{pmatrix} 1 & W \\ 0 & 1 \end{pmatrix}\begin{pmatrix} Q \\ E \end{pmatrix}, \tag{A17}$$

where the matrices R and M parametrize a linear transformation among the physical and evanescent operators Q and E, respectively, W parametrizes the addition of multiples of evanescent operators to the physical operators, and U and V parametrize the addition of multiples of ϵ and ϵ^2 times physical operators to the evanescent operators, respectively. We apply a transformation of the same form to the dimension-eight operators, where we denote the corresponding matrices by a tilde, as before. The finite renormalization constants can now be determined by requiring that an effective amplitude of the form $C_iZ_{ij}\langle Q_j\rangle + (\tilde{C}_l\tilde{Z}_{lk} + C_iC_j\hat{Z}_{ij,k})\langle\tilde{Q}_k\rangle$ be invariant under the basis transformation and be renormalized according to the $\overline{\mathrm{MS}}$ prescription.

Let us start with the anomalous dimension matrices for the mixing of dimension-six into dimension-six operators. The finite renormalization induced by the change (A17) is given by [4,13]

$$\begin{aligned} Z'^{(1,0)}_{QQ} &= R\left[WZ^{(1,0)}_{EQ} - \left(Z^{(1,1)}_{QE} + WZ^{(1,1)}_{EE} - \frac{1}{2}\gamma^{(0)}W\right)U\right]R^{-1}, \\ Z'^{(2,0)}_{QQ} &= -R\left(Z^{(2,1)}_{QE}U + Z^{(2,2)}_{QE}V - \frac{1}{2}Z^{(1,1)}_{QE}V\gamma^{(0)}\right)R^{-1}, \end{aligned} \tag{A18}$$

where

$$Z^{(2,2)}_{QE} = \frac{1}{2}\left(Z^{(1,1)}_{QE}Z^{(1,1)}_{EE} + \frac{1}{2}\gamma^{(0)}Z^{(1,1)}_{QE} - \beta_0Z^{(1,1)}_{QE}\right). \tag{A19}$$

We have set W to zero in the second line of Eq. (A18) as these terms are not needed in our work. We now find the transformation law for the anomalous dimension matrices in a straightforward manner using Eqs. (A10) to (A12):

$$\begin{aligned} \gamma'^{(0)} &= R\gamma^{(0)}R^{-1}, \\ \gamma'^{(1)} &= R\gamma^{(1)}R^{-1} - [Z'^{(1,0)}_{QQ}, \gamma'^{(0)}] - 2\beta_0Z'^{(1,0)}_{QQ}, \\ \gamma'^{(2)} &= R\gamma^{(2)}R^{-1} - [Z'^{(2,0)}_{QQ}, \gamma'^{(0)}] - [Z'^{(1,0)}_{QQ}, \gamma'^{(1)}] + [Z'^{(1,0)}_{QQ}, \gamma'^{(0)}]Z'^{(1,0)}_{QQ} - 4\beta_0Z'^{(2,0)}_{QQ} - 2\beta_1Z'^{(1,0)}_{QQ} + 2\beta_0(Z'^{(1,0)}_{QQ})^2. \end{aligned} \tag{A20}$$

The Wilson coefficients change according to

$$C'(\mu) = \left[1 + \frac{\alpha_s(\mu)}{4\pi}Z'^{(1,0)}_{QQ} + \left(\frac{\alpha_s(\mu)}{4\pi}\right)^2Z'^{(2,0)}_{QQ}\right]^T \times (R^{-1})^TC(\mu). \tag{A21}$$

Clearly, the transformation law of the anomalous dimension matrix describing the mixing among the dimension-eight operators themselves is given by a formula completely analogous to (A20). In order to find the transformation law of the anomalous dimension tensor, describing the mixing of dimension-six into dimension-eight operators, and of the dimension-eight Wilson coefficients, we apply the same method as above. In addition to the finite renormalization constants (A18), we now get extra finite contributions to $\hat{Z}$:

$$\hat{Z}'^{(1,0)}_{ij,k} = R_{im}R_{jn}(\hat{Z}^{(1,1)}_{mn,l}\tilde{W}_{ll'}\tilde{U}_{l'p} - \hat{Z}^{(1,1)}_{mn,l}\tilde{U}_{lp} + W_{ml}\hat{Z}^{(1,0)}_{ln,p} + W_{nl}\hat{Z}^{(1,0)}_{ml,p} - W_{il}\hat{Z}^{(1,1)}_{ln,m}\tilde{U}_{mp} - W_{nl}\hat{Z}^{(1,1)}_{il,m}\tilde{U}_{mp})\tilde{R}^{-1}_{pk}. \tag{A22}$$

[7]Note that additional finite contributions arise if we include the factor of m_c^2/g^2 in the definition of the dimension-eight operators.

Here the indices i, j, and k correspond to physical operators only. These expressions have never been given explicitly in the literature before. The anomalous dimension tensor then transforms according to

$$\gamma^{\prime(0)}_{ij,k} = R_{im} R_{jn} \gamma^{(0)}_{mn,l} \tilde{R}^{-1}_{lk}, \tag{A23}$$

$$\begin{aligned}\gamma^{\prime(1)}_{ij,k} = {} & R_{im} R_{jn} \gamma^{(1)}_{mn,l} \tilde{R}^{-1}_{lk} + \hat{Z}^{\prime(1,0)}_{ij,l} \tilde{\gamma}^{\prime(0)}_{lk} + 2\hat{Z}^{\prime(1,0)}_{ij,k} \beta_0 \\ & + \hat{\gamma}^{\prime(0)}_{ij,l} \tilde{Z}^{\prime(1,0)}_{lk} - \{\gamma^{\prime(0)}_{il} \delta_{jm} + \delta_{il} \gamma^{\prime(0)}_{jm}\} \hat{Z}^{\prime(1,0)}_{lm,k} \\ & - \{Z^{\prime(1,0)}_{il} \delta_{jm} + \delta_{il} Z^{\prime(1,0)}_{jm}\} \hat{\gamma}^{\prime(0)}_{lm,k},\end{aligned} \tag{A24}$$

as can be derived easily from Eqs. (A13) and (A14). A special case of these formulas has been derived in Ref. [15]. Using the definition (A2), we see that the dimension-eight Wilson coefficients transform as

$$\begin{aligned}\tilde{C}^{\prime}_k(\mu) = {} & \tilde{C}_i(\mu) \tilde{R}^{-1}_{ij} \left[\delta_{jk} + \frac{\alpha_s(\mu)}{4\pi} \tilde{Z}^{\prime(1,0)}_{jk} \right] \\ & - C_i(\mu) R^{-1}_{im} C_j(\mu) R^{-1}_{jn} \left[\frac{\alpha_s(\mu)}{4\pi} \hat{Z}^{\prime(1,0)}_{mn,k} \right].\end{aligned} \tag{A25}$$

1. Transformation to the traditional operator basis

The calculation of the NLO QCD corrections to η_{ct} in [7] has been performed in a different basis for the physical operators than the one chosen by us. It is given by

$$\begin{aligned}Q^{\prime qq^{\prime}}_1 &= (\bar{s}^{\alpha}_L \gamma_{\mu} q^{\alpha}_L) \otimes (\bar{q}^{\prime\beta}_L \gamma^{\mu} d^{\beta}_L), \\ Q^{\prime qq^{\prime}}_2 &= (\bar{s}^{\alpha}_L \gamma_{\mu} q^{\beta}_L) \otimes (\bar{q}^{\prime\beta}_L \gamma^{\mu} d^{\alpha}_L), \\ Q^{\prime}_3 &= (\bar{s}^{\alpha}_L \gamma_{\mu} d^{\alpha}_L) \otimes \sum_q (\bar{q}^{\prime\beta}_L \gamma^{\mu} q^{\beta}_L), \\ Q^{\prime}_4 &= (\bar{s}^{\alpha}_L \gamma_{\mu} d^{\beta}_L) \otimes \sum_q (\bar{q}^{\prime\beta}_L \gamma^{\mu} q^{\alpha}_L), \\ Q^{\prime}_5 &= (\bar{s}^{\alpha}_L \gamma_{\mu} d^{\alpha}_L) \otimes \sum_q (\bar{q}^{\prime\beta}_R \gamma^{\mu} q^{\beta}_R), \\ Q^{\prime}_6 &= (\bar{s}^{\alpha}_L \gamma_{\mu} d^{\beta}_L) \otimes \sum_q (\bar{q}^{\prime\beta}_R \gamma^{\mu} q^{\alpha}_R).\end{aligned} \tag{A26}$$

Note that we have expressed the operators in terms of left- and right-handed fermion fields, in contrast to the definition used in [7]. The evanescent operators chosen in [7] are equivalent to the following set of operators:

$$\begin{aligned}E^{\prime qq^{\prime}(1)}_1 &= (\bar{s}^{\alpha}_L \gamma_{\mu_1\mu_2\mu_3} q^{\alpha}_L) \otimes (\bar{q}^{\prime\beta}_L \gamma^{\mu_1\mu_2\mu_3} d^{\beta}_L) - (16 - 4\epsilon) Q^{\prime qq^{\prime}}_1, \\ E^{\prime qq^{\prime}(1)}_2 &= (\bar{s}^{\alpha}_L \gamma_{\mu_1\mu_2\mu_3} q^{\beta}_L) \otimes (\bar{q}^{\prime\beta}_L \gamma^{\mu_1\mu_2\mu_3} d^{\alpha}_L) - (16 - 4\epsilon) Q^{\prime qq^{\prime}}_2, \\ E^{\prime(1)}_3 &= (\bar{s}^{\alpha}_L \gamma_{\mu_1\mu_2\mu_3} d^{\alpha}_L) \otimes \sum_q (\bar{q}^{\prime\beta}_L \gamma^{\mu_1\mu_2\mu_3} q^{\beta}_L) - (16 - 4\epsilon) Q^{\prime}_3, \\ E^{\prime(1)}_4 &= (\bar{s}^{\alpha}_L \gamma_{\mu_1\mu_2\mu_3} d^{\beta}_L) \otimes \sum_q (\bar{q}^{\prime\beta}_L \gamma^{\mu_1\mu_2\mu_3} q^{\alpha}_L) - (16 - 4\epsilon) Q^{\prime}_4, \\ E^{\prime(1)}_5 &= (\bar{s}^{\alpha}_L \gamma_{\mu_1\mu_2\mu_3} d^{\alpha}_L) \otimes \sum_q (\bar{q}^{\prime\beta}_R \gamma^{\mu_1\mu_2\mu_3} q^{\beta}_R) - (4 + 4\epsilon) Q^{\prime}_5, \\ E^{\prime(1)}_6 &= (\bar{s}^{\alpha}_L \gamma_{\mu_1\mu_2\mu_3} d^{\beta}_L) \otimes \sum_q (\bar{q}^{\prime\beta}_R \gamma^{\mu_1\mu_2\mu_3} q^{\alpha}_R) - (4 + 4\epsilon) Q^{\prime}_6.\end{aligned} \tag{A27}$$

It turns out that in order to transform from our operator basis to the traditional one the following four evanescent operators must be introduced at the one-loop level in addition to the evanescent operators given in Eq. (2.10) (see Ref. [4]):

$$\begin{aligned}E^{(1)}_5 &= (\bar{s}_L \gamma_{\mu} d_L) \otimes \sum_q (\bar{q} \gamma^{\mu} \gamma_5 q) - \frac{5}{3} Q_3 + \frac{1}{6} Q_5, \\ E^{(1)}_6 &= (\bar{s}_L \gamma_{\mu} T^a d_L) \otimes \sum_q (\bar{q} \gamma^{\mu} \gamma_5 T^a q) - \frac{5}{3} Q_4 + \frac{1}{6} Q_6, \\ E^{(1)}_7 &= (\bar{s}_L \gamma_{\mu_1\mu_2\mu_3} d_L) \otimes \sum_q (\bar{q} \gamma^{\mu_1\mu_2\mu_3} \gamma_5 q) - \frac{32}{3} Q_3 + \frac{5}{3} Q_5, \\ E^{(1)}_8 &= (\bar{s}_L \gamma_{\mu_1\mu_2\mu_3} T^a d_L) \otimes \sum_q (\bar{q} \gamma^{\mu_1\mu_2\mu_3} \gamma_5 T^a q) - \frac{32}{3} Q_4 + \frac{5}{3} Q_6.\end{aligned} \tag{A28}$$

The transformation matrices R, M, W, and U representing the basis transformation according to Eq. (A17), as well as the finite renormalization induced by this transformation, can be found in [4]. The parts of the transformation matrices relevant to us are given by[8]

[8] An additional rotation must be performed in order to change to the "diagonal" operator basis. This does not affect the finite renormalization.

$$R = \begin{pmatrix} 2 & \frac{1}{3} & 0 & 0 & 0 & 0 \\ 0 & 1 & 0 & 0 & 0 & 0 \\ 0 & 0 & -\frac{1}{3} & 0 & \frac{1}{12} & 0 \\ 0 & 0 & -\frac{1}{9} & -\frac{2}{3} & \frac{1}{36} & \frac{1}{6} \\ 0 & 0 & \frac{4}{3} & 0 & -\frac{1}{12} & 0 \\ 0 & 0 & \frac{4}{9} & \frac{8}{3} & -\frac{1}{36} & -\frac{1}{6} \end{pmatrix},$$

$$M = \begin{pmatrix} 2 & \frac{1}{3} & 0 & 0 & 0 & 0 & 0 & 0 \\ 0 & 1 & 0 & 0 & 0 & 0 & 0 & 0 \\ 0 & 0 & 0 & 0 & 8 & 0 & -\frac{1}{2} & 0 \\ 0 & 0 & 0 & 0 & \frac{8}{3} & 16 & -\frac{1}{6} & -1 \\ 0 & 0 & 0 & 0 & -2 & 0 & \frac{1}{2} & 0 \\ 0 & 0 & 0 & 0 & -\frac{2}{3} & -4 & \frac{1}{6} & 1 \end{pmatrix}, \tag{A29}$$

$$W = \begin{pmatrix} 0 & 0 & 0 & 0 & 0 & 0 & 0 & 0 \\ 0 & 0 & 0 & 0 & 0 & 0 & 0 & 0 \\ 0 & 0 & 0 & 0 & 0 & 0 & 0 & 0 \\ 0 & 0 & 0 & 0 & 0 & 0 & 0 & 0 \\ 0 & 0 & 0 & 0 & -6 & 0 & 0 & 0 \\ 0 & 0 & 0 & 0 & 0 & -6 & 0 & 0 \end{pmatrix},$$

$$U = \begin{pmatrix} 0 & 0 & 0 & 0 & 0 & 0 \\ 0 & 0 & 0 & 0 & 0 & 0 \\ 0 & 0 & -112 & 0 & 16 & 0 \\ 0 & 0 & 0 & -112 & 0 & 16 \\ 0 & 0 & -\frac{10}{9} & 0 & \frac{1}{9} & 0 \\ 0 & 0 & 0 & -\frac{10}{9} & 0 & \frac{1}{9} \\ 0 & 0 & -\frac{136}{9} & 0 & \frac{10}{9} & 0 \\ 0 & 0 & 0 & -\frac{136}{9} & 0 & \frac{10}{9} \end{pmatrix}, \tag{A30}$$

whereas the matrix V vanishes. They correspond to the bases

$$\begin{aligned} Q' &= (Q_1'^{qq'}, Q_2'^{qq'}, Q_3', \ldots, Q_6'), \\ E' &= (E_1'^{qq'(1)}, E_2'^{qq'(1)}, E_3'^{(1)}, \ldots, E_6'^{(1)}), \end{aligned} \tag{A31}$$

and

$$\begin{aligned} Q &= (Q_1^{qq'}, Q_2^{qq'}, Q_3, \ldots, Q_6), \\ E &= (E_1^{qq'(1)}, E_2^{qq'(1)}, E_3^{(1)}, \ldots, E_8^{(1)}) \end{aligned} \tag{A32}$$

in the notation of (A17). The one-loop contribution to the finite renormalization in the dimension-six sector is given by

$$Z_{QQ}^{\prime(1,0)} = \begin{pmatrix} 0 & 0 & 0 & 0 & 0 & 0 \\ 0 & 0 & 0 & 0 & 0 & 0 \\ 0 & 0 & \frac{178}{27} & -\frac{34}{9} & -\frac{164}{27} & \frac{20}{9} \\ 0 & 0 & 1-\frac{f}{9} & \frac{f}{3}-\frac{25}{3} & -\frac{f}{9}-2 & \frac{f}{3}+6 \\ 0 & 0 & -\frac{160}{27} & \frac{16}{9} & \frac{146}{27} & -\frac{2}{9} \\ 0 & 0 & \frac{f}{9}-2 & 6-\frac{f}{3} & \frac{f}{9}+3 & -\frac{f}{3}-\frac{11}{3} \end{pmatrix}. \tag{A33}$$

The finite renormalization relevant for the mixing of dimension-six into dimension-eight operators has never been calculated before. We find

$$\hat{Z}^{\prime(1,0),T}_{QQ,\tilde{Q}_7} = \begin{pmatrix} 0 & 0 & -20 & -\frac{20}{3} & 20 & \frac{20}{3} \\ 0 & 0 & -\frac{20}{3} & -\frac{20}{3} & \frac{20}{3} & \frac{20}{3} \end{pmatrix}. \tag{A34}$$

2. Transformation to the diagonal operator basis

Here we describe the change from the operator basis, where the current-current operators are defined as in Ref. [4,12], to the diagonal basis, as defined in [13] (and in this work). The transformation matrices R, M, U, and V in the notation of (A17) are now given by [4,13][9]

$$R = \begin{pmatrix} 1 & \frac{2}{3} & 0 & 0 & 0 & 0 \\ -1 & \frac{1}{3} & 0 & 0 & 0 & 0 \\ 0 & 0 & 1 & 0 & 0 & 0 \\ 0 & 0 & 0 & 1 & 0 & 0 \\ 0 & 0 & 0 & 0 & 1 & 0 \\ 0 & 0 & 0 & 0 & 0 & 1 \end{pmatrix},$$

$$M_{ij} = \begin{cases} 1, & i = j, \\ 20, & (i,j) \in \{(9,1),(10,2)\}, \\ 0, & \text{otherwise}; \end{cases}$$

$$U_{ij} = \begin{cases} 4, & (i,j) \in \{(1,1),(2,2)\}, \\ 144, & (i,j) \in \{(5,1),(6,2)\}, \\ 0, & \text{otherwise}; \end{cases} \tag{A35}$$

$$V_{ij} = \begin{cases} 4, & (i,j) \in \{(1,1),(2,2)\}, \\ \frac{3712}{25}, & (i,j) = (5,1), \\ \frac{8032}{25}, & (i,j) = (6,2), \\ 0, & \text{otherwise}; \end{cases}$$

and the matrix W vanishes. These matrices correspond to the following bases of operators (the roles of the primed and unprimed set of operators is reversed with respect to Ref. [13]):

$$Q' = (Q_+, Q_-), \qquad E' = (E_1^{qq'}, E_2^{qq'}, E_3^{qq'}, E_4^{qq'}), \tag{A36}$$

and

$$Q = (Q_1, Q_2), \qquad E = (E_1^{(1)}, E_2^{(1)}, E_1^{(2)}, E_2^{(2)}). \tag{A37}$$

All necessary renormalization constants can be found in Ref. [4]. The finite renormalization is then given by

[9]Here we have implicitly corrected some typos in Ref. [13].

$$Z_{QQ}^{\prime(1,0)} = \begin{pmatrix} -\frac{5}{3} & -\frac{8}{9} & 0 & 0 & 0 & 0 \\ -4 & 0 & 0 & 0 & 0 & 0 \\ 0 & 0 & 0 & 0 & 0 & 0 \\ 0 & 0 & 0 & 0 & 0 & 0 \\ 0 & 0 & 0 & 0 & 0 & 0 \\ 0 & 0 & 0 & 0 & 0 & 0 \end{pmatrix}, \qquad Z_{QQ}^{\prime(2,0)} = \begin{pmatrix} -\frac{29123}{900} - \frac{25}{54} f & \frac{17}{135} - \frac{20}{81} f & 0 & \frac{11}{27} & 0 & 0 \\ -\frac{343}{30} - \frac{10}{9} f & -\frac{498}{25} & 0 & -\frac{4}{9} & 0 & 0 \\ 0 & 0 & 0 & 0 & 0 & 0 \\ 0 & 0 & 0 & 0 & 0 & 0 \\ 0 & 0 & 0 & 0 & 0 & 0 \\ 0 & 0 & 0 & 0 & 0 & 0 \end{pmatrix}. \tag{A38}$$

[1] J. H. Christenson, J. W. Cronin, V. L. Fitch, and R. Turlay, Phys. Rev. Lett. **13**, 138 (1964).
[2] K. Nakamura *et al.* (Particle Data Group), J. Phys. G **37**, 075021 (2010).
[3] A. J. Buras, D. Guadagnoli, and G. Isidori, Phys. Lett. B **688**, 309 (2010).
[4] M. Gorbahn and U. Haisch, Nucl. Phys. **B713**, 291 (2005).
[5] A. I. Vainshtein, V. I. Zakharov, V. A. Novikov, and M. A. Shifman, Yad. Fiz. **23**, 1024 (1976) [Sov. J. Nucl. Phys. **23**, 540 (1977)]; F. J. Gilman and M. B. Wise, Phys. Rev. D **27**, 1128 (1983); J. M. Flynn, Mod. Phys. Lett. A **5**, 877 (1990); A. Datta, J. Frohlich, and E. A. Paschos, Z. Phys. C **46**, 63 (1990).
[6] S. Herrlich and U. Nierste, Nucl. Phys. **B419**, 292 (1994).
[7] S. Herrlich and U. Nierste, Nucl. Phys. **B476**, 27 (1996).
[8] A. J. Buras, M. Jamin, and P. H. Weisz, Nucl. Phys. **B347**, 491 (1990).
[9] J. Laiho, E. Lunghi, and R. S. Van de Water, Phys. Rev. D **81**, 034503 (2010).
[10] O. Cata and S. Peris, J. High Energy Phys. 07 (2004) 079.
[11] J. Brod and M. Gorbahn (unpublished).
[12] K. G. Chetyrkin, M. Misiak, and M. Munz, Nucl. Phys. **B520**, 279 (1998).
[13] A. J. Buras, M. Gorbahn, U. Haisch, and U. Nierste, J. High Energy Phys. 11 (2006) 002.
[14] C. Bobeth, M. Misiak, and J. Urban, Nucl. Phys. **B574**, 291 (2000).
[15] S. Herrlich and U. Nierste, Nucl. Phys. **B455**, 39 (1995).
[16] K. G. Chetyrkin, M. Misiak, and M. Munz, Nucl. Phys. **B518**, 473 (1998).
[17] H. Simma, Z. Phys. C **61**, 67 (1994).
[18] S. A. Larin, Phys. Lett. B **303**, 113 (1993).
[19] O. V. Tarasov (unpublished).
[20] O. V. Tarasov, A. A. Vladimirov, and A. Y. Zharkov, Phys. Lett. **B93**, 429 (1980).
[21] S. A. Larin and J. A. M. Vermaseren, Phys. Lett. B **303**, 334 (1993).
[22] W. Wetzel, Nucl. Phys. **B196**, 259 (1982).
[23] W. Bernreuther and W. Wetzel, Nucl. Phys. **B197**, 228 (1982); **B513**, 758(E) (1998).
[24] W. Bernreuther, Ann. Phys. (N.Y.) **151**, 127 (1983).
[25] K. G. Chetyrkin, B. A. Kniehl, and M. Steinhauser, Nucl. Phys. **B510**, 61 (1998).
[26] P. Nogueira, J. Comput. Phys. **105**, 279 (1993).
[27] R. Harlander, T. Seidensticker, and M. Steinhauser, Phys. Lett. B **426**, 125 (1998); T. Seidensticker, arXiv:hep-ph/9905298.
[28] M. Steinhauser, Comput. Phys. Commun. **134**, 335 (2001).
[29] J. A. M. Vermaseren, arXiv:math-ph/0010025.
[30] F. V. Tkachov, Phys. Lett. **B100**, 65 (1981).
[31] K. G. Chetyrkin and F. V. Tkachov, Nucl. Phys. **B192**, 159 (1981).
[32] A. I. Davydychev and J. B. Tausk, Nucl. Phys. **B397**, 123 (1993).
[33] T. Hahn, Comput. Phys. Commun. **140**, 418 (2001).
[34] CDF Collaboration and D0 Collaboration, arXiv:1007.3178.
[35] M. Antonelli *et al.* (FlaviaNet Working Group on Kaon Decays), Nucl. Phys. B, Proc. Suppl. **181-182**, 83 (2008).
[36] K. G. Chetyrkin, J. H. Kuhn, A. Maier, P. Maierhofer, P. Marquard, M. Steinhauser, and C. Sturm, Phys. Rev. D **80**, 074010 (2009).
[37] K. G. Chetyrkin, J. H. Kühn, and M. Steinhauser, Comput. Phys. Commun. **133**, 43 (2000).
[38] G. Buchalla, A. J. Buras, and M. E. Lautenbacher, Rev. Mod. Phys. **68**, 1125 (1996).
[39] A. J. Buras and D. Guadagnoli, Phys. Rev. D **78**, 033005 (2008).
[40] A. J. Buras, M. Jamin, M. E. Lautenbacher, and P. H. Weisz, Nucl. Phys. **B370**, 69 (1992); **B375**, 501 (1992).
[41] M. Ciuchini, E. Franco, G. Martinelli, and L. Reina, Nucl. Phys. **B415**, 403 (1994).